Stony Brook University

Metalloproteinase Activators of Notch Signaling in Development and Pancreatic Disease

A Dissertation Presented

by

Eric Thomas Sawey

to

The Graduate School

in Partial Fulfillment of the

Requirements

for the Degree of

Doctor of Philosophy

in

Molecular and Cellular Pharmacology

Stony Brook University

May 2008

Stony Brook University

The Graduate School

Eric Thomas Sawey

We, the dissertation committee for the above candidate for the

Doctor of Philosophy degree, hereby recommend

acceptance of this dissertation.

Howard Crawford, PhD – Dissertation Advisor
Assistant Professor, Department of Pharmacological Sciences

Robert Haltiwanger, PhD – Chairperson of Defense
Professor, Department of Biochemistry and Cell Biology

Stella Tsirka, PhD
Associate Professor, Department of Pharmacological Sciences

Stanley Zucker, PhD
Professor, Department of Medicine

This dissertation is accepted by the Graduate School

Lawrence Martin
Dean of the Graduate School

Abstract of the Dissertation

Metalloproteinase Activators of Notch Signaling in Development and Pancreatic Disease

by

Eric Thomas Sawey

Doctor of Philosophy

in

Molecular and Cellular Pharmacology

Stony Brook University

2008

Notch signaling is involved in numerous cell-signaling events, both during development and disease. We used an *in vitro* model of pancreatic disease to examine metalloproteinase influences on Notch activity. Acinar-to-ductal metaplasia in the pancreas is associated with an increased risk for tumorigenesis. Examination of this process *in vitro* has shown that primary acinar cells, in response to EGF receptor ligands, can transdifferentiate into duct-like epithelia, in a Notch pathway-dependent manner. Matrix Metalloproteinase 7 (MMP-7) is a proteinase expressed in most metaplastic epithelia *in vivo*. Here, we show that *in vitro* acinar transdifferentiation is mediated by MMP-7's ability to activate Notch. Besides being necessary for acinar transdifferentiation, it was found that MMP-7 activity was sufficient to induce the process, indicating that molecular signals capable of initiating MMP-7 expression also have the potential to induce formation of metaplastic epithelia in the pancreas.

A Disintegrin and Metalloproteinase 10 (ADAM-10) has been shown to be required for Notch activity, however it is unclear where along the Notch pathway ADAM-10 functions. Here, we introduce a conditional ADAM-10 knockout mouse to further dissect its role in Notch signaling. We found that ADAM-10 activity is essential for the extracellular processing of Notch, but not for the intracellular processing necessary for proper Notch maturation. We also identified various phenotypes associated with defective Notch signaling in the embryo, skin and brain of the knockout mouse.

Dedication

For my grandfather, Daniel Pastore;

my #1 fan and best friend.

Table of Contents

List of Abbreviations

Ad— adenovirus
ADAM—A Disintegrin and Metalloproteinase
ADM— acinar-to-ductal metaplasia
CBP— calmodulin-binding peptide
CK-19— cytokeratin 19
CMV— cytomegalovirus
COX-2— cyclooxygenase 2
CP— chronic pancreatitis
CSL— CBF-1/RBP-Jκ, Su(H), Lag-1
ECD— extracellular domain
ECM— extracellular matrix
EGF— epidermal growth factor
EL— elastase
ER— estrogen receptor
DAPI— 4'6-diamidino-2-phenylindole-2HCl
DMEM— Dulbecco's Modified Eagle Medium
FasL— Fas Ligand
FBS— fetal bovine serum
GFP— green fluorescent protein
GSI— γ-secretase inhibitor
HB-EGF— heparin-binding epidermal growth factor
HBSS— Hanks' Balanced Salt Solution
HES— Hairy Enhancer of Split
ICD— intracellular domain
IL-6— interleukin 6
iNOS— inducible nitric oxide synthase
LPS— lipopolysaccharide
MDL— metaplastic duct lesion
MEF— murine embryonic fibroblast
MMP— matrix metalloproteinase
MOI— multiplicity of infection
MT— metallothionein
PanIN— pancreatic intraepithelial neoplasia
PBS— phosphate buffered saline
PBSMT— PBS + milk + Tween-20
PCR— polymerase chain reaction
PDAC— pancreatic ductal adenocarcinoma
rMMP-7— recombinant MMP-7
RTC— rat tail collagen
RT-PCR— reverse transcriptase-polymerase chain reaction
TGF-α— transforming growth factor α
TNF-α— tumor necrosis factor α
Tyr— tyrosinase

List of Figures

Acknowledgements

I would like to thank the members of the Crawford lab: Howard Crawford, Yan Song, Christine Ardito, Lorenzo Bombardelli, Johnny Johnson, Ninche Alston and Courtney Briggs for their suggestions and friendship.

Some material is reprinted with permission from articles published in PNAS and Cell Cycle.

Permission from PNAS was granted by Diane Sullenberger (Executive Editor, PNAS): Authors need not obtain permission for the following uses of material they have published in PNAS: (1) to use their original figures or tables in their future works; (2) to make copies of their papers for their classroom teaching; or **(3) to include their papers as part of their dissertations**.

Permission from Cell Cycle was granted through the copyright agreement: Landes Bioscience/Eurekah.com grant back to the Author the non-exclusive rights to **(a) use of all or part of the Contribution (after publication in the Journal) in any book or article written by the Author(s) (including a PhD thesis or dissertation)** and (b) make photocopies of all or part of the Contribution for use by the Author(s) in classroom teaching.

Publications

Sawey ET, Johnson JA, Crawford HC. Matrix metalloproteinase 7 controls pancreatic acinar cell transdifferentiation by activating the Notch signaling pathway. Proc Natl Acad Sci USA 2007;104(49):19327-32.

Sawey ET, Crawford HC. Metalloproteinases and cell fate: Notch just ADAMs anymore. Cell Cycle 2008;7(5):566-569.

Introduction

Significance

Pancreatic ductal adenocarcinoma (PDAC), the most common form of pancreatic cancer, is a devastating disease that is expected to affect 37,680 Americans in 2008 [1]. Representing only 2.3% of all cancer cases in the United States, pancreatic cancer is still the 4th leading cause of cancer death among both males and females. Patients with this disease have a 5-year survival rate of 5% with a median survival time of less than one year. Characteristically late diagnosis results in resistance to conventional treatments.

One factor that predisposes patients to pancreatic cancer is chronic inflammation, or chronic pancreatitis (CP). Some risk factors associated with CP are smoking, high-fat diet and excessive alcohol use. Patients with nonhereditary CP are 16 times more likely to develop PDAC over their lifetimes [2], with the relative risk increasing to 50-fold for hereditary CP patients [3]. Some epithelial responses to chronic inflammation, such as expression of the inducible nitric oxide synthase (iNOS) and tumor necrosis factor-α (TNF-α) [4], have been shown to lead to genetic mutations that can induce neoplastic transformation. Cyclooxygenase-2 (COX-2) expression can also be induced by inflammation and can initiate a proliferative response [5].

Epithelial metaplasia, the transition from one predominant differentiated epithelial cell type to another, is commonly found at sites of chronic inflammation, including pancreatitis [2, 3, 6]. The characteristic epithelial metaplasia of both CP and PDAC is acinar-to-ductal metaplasia (ADM). Pathological evidence strongly suggests that PDAC arises from premalignant lesions known as pancreatic intraepithelial neoplasia (PanIN) [7]. Although there is evidence that PanINs arise from a preexisting stem cell population [8], a second possible preneoplastic lesion is the metaplastic duct lesion (MDL). The fact that MDLs are associated with CP, a known risk factor for PDAC, and gradually become a more substantial proportion of the pancreatic epithelia in patients over time leads to the hypothesis that these structures may act as tumor precursors.

This idea is supported by transgenic mouse models in which transforming growth factor-α (TGF-α) is overexpressed in the exocrine pancreas. When TGF-α is directed to the exocrine pancreas under the control of either the elastase promoter (EL-TGF-α) [9] or the metallothionein promoter (MT-TGF-α) [10], it induces ADM and, over a period of about a year, 10% of these mice develop PanINs and PDAC [11]. These models support the conclusions from epidemiological studies: that the metaplastic duct lesions are preneoplastic. With ADM being a common link between both pancreatitis and PDAC, it is of interest to identify proteins involved in this transition.

Notch

One protein identified as being required for ADM is the transmembrane receptor Notch [12]. The Notch pathway is involved in numerous cell-signaling events, both during development and disease. Typically, Notch receptors (Notch 1–4) are activated upon interaction with one of their ligands (Jagged or Delta-like) on an adjacent cell (for review, see [13]) (Fig. 1). Upon ligation, the extracellular portion of Notch is cleaved by a metalloproteinase followed by intramembrane cleavage by a presenilin-dependent γ-secretase. The newly liberated Notch intracellular domain (Notch-ICD) translocates to the nucleus where it interacts with the DNA-binding protein CSL [CBF-1/RBP-Jκ, Su(H), Lag-1], converting it from transcriptional repressor to transcriptional activator. Notch-ICD–CSL complexes activate transcription of genes, such as Hairy Enhancer of Split (*hes1*), which function to block cellular differentiation. Notch blocks pancreatic acinar cell differentiation [14, 15] through the inactivation of PTF1, a transcription factor complex required for acinar differentiation, by Notch-ICD displacing Ptf1a from CSL [16], as well as by HES1 directly interacting with and blocking Ptf1a function [17].

Notch receptors and some of their ligands (Jagged-1 and -2) are upregulated in patient samples of PDAC [12]. An *in vitro* model of ADM has been established where primary acinar cell explants are embedded in three-dimensional fibrillar collagen and treated with TGF-α [18]. In this system, acinar cell differentiation is progressively lost with a reciprocal increase in duct cell differentiation, as determined by expression of cell-specific molecular markers. Recent studies have shown that this *in vitro* ADM represents a true cellular transdifferentiation, in which cells pass through a nestin-positive intermediate [19]. Over the course of the culture, Notch target genes including *hes1* and *hey1* are upregulated. In addition, when primary acinar cells were infected with an adenoviral vector encoding the activated intracellular domain of either Notch-1 or Notch-2, the cells underwent the metaplastic transition to a ductal morphology, independent of TGF-α [12]. These results showed that Notch functions downstream of TGF-α, and that Notch pathway activation is sufficient to induce this early event in pancreatic tumorigenesis.

A role for Notch in tumorigenesis is increasingly apparent. The multiple intestinal neoplasia (Apc^{Min}) mouse model takes advantage of a constitutively active Wnt pathway to cause spontaneous adenoma formation in the small intestine [20]. In one study, Notch function was inhibited by injecting Apc^{Min} mice with a pharmacological inhibitor of γ-secretase [21]. The result was a conversion of proliferative, undifferentiated tumor cells into post-mitotic, differentiated goblet cells. Therefore, inhibiting Notch in this model caused tumors to differentiate.

MMP-7

The matrix metalloproteinases (MMPs) comprise a family of 23 extracellular, zinc-dependent proteinases frequently expressed in cancer [22]. MMPs can collectively degrade all components of the extracellular matrix (ECM), suggesting a role in tumor invasion. However, evidence derived from mouse genetics has shown that MMPs

contribute to multiple stages of tumor progression, including tumorigenesis and tumor growth, often by cleaving non-ECM substrates [23].

MMP-7 is distinguished from the other MMPs in that it has a minimal domain structure, consisting of the zinc-binding site in the catalytic domain and the cysteine-switch region in the pro domain responsible for maintaining enzyme latency. Other MMPs contain additional domains that are involved in substrate specificity, inhibitor binding, matrix binding and cell-surface localization. Another characteristic that sets MMP-7 apart from the other MMPs is its expression in glandular epithelial cells, compared to the more common expression of other MMPs in tissue mesenchyme. The epithelially-restricted expression pattern of MMP-7 includes its expression in human adenocarcinomas. MMP-7 is expressed by the cells of breast, stomach, colon, prostate, upper aerodigestive tract, and lung tumors [24], and by associated metaplasia, including in colon [25], stomach [25], and the majority of PDACs, at all PanIN stages, and in 100% of tumor-associated MDLs [26]. Animal models have supported a role for MMP-7 in tumorigenesis and early tumor growth. In Apc^{Min} mice, MMP-7 deficiency inhibits intestinal tumor formation [27]. Conversely, overexpression of MMP-7 in the mammary gland in the MMTV-Neu transgenic background accelerates tumor formation [28]. Although its role in PDAC has not been directly addressed, in the pancreatic ductal ligation mouse model of CP, in which the main pancreatic duct is sutured closed to recreate the ductal obstruction and digestive enzyme build-up in the pancreatic tail that is seen in human CP, there is limited acinar cell loss and few signs of ductal metaplasia, compared to the high rate of ADM in wild-type mice [26]. Together, these data suggest that MMP-7 acts early in adenoma progression, perhaps in tumorigenesis itself.

Consistent with MMP-7's role in early tumor formation, a number of MMP-7 substrates have been identified. Interestingly, MMP-7's substrates are identical to substrates also identified as ADAM (A Disintegrin And Metalloproteinase) substrates. One such substrate is heparin-binding epidermal growth factor (HB-EGF). MMP-7 releases HB-EGF from the plasma membrane which has been shown to enhance cellular proliferation and contribute to apoptotic resistance [29]. Many MMP-7 substrates have been linked to aspects of PDAC progression, including syndecan-1 [30, 31], E-cadherin [32, 33], and TNF-α [34, 35]. In mouse CP, Fas Ligand (FasL) was determined to be a relevant *in vivo* MMP-7 substrate that controls acinar cell apoptosis [26]. However, these data do not provide a satisfactory explanation as to why MDL formation is inhibited in MMP-$7^{-/-}$ mice. Indeed, given the inhibition of all aspects of CP progression in this model, including inflammation, fibrosis, apoptosis, and metaplasia, it was impossible to determine whether the processes are independent of one another.

ADAM-10's Role in Notch Signaling

ADAMs are multifunctional proteins involved in the proteolytic processing of other transmembrane proteins, regulating cell adhesion and other cell signaling events. ADAM-10 (Kuzbanian, MADM) is a transmembrane ADAM that can cleave amyloid precursor protein at the α-secretase processing site [36] and may be involved in degrading the extracellular matrix, by cleaving type IV collagen, for example [37]. In addition to being identified as the main sheddase of two membrane proteins, epidermal growth factor

(EGF) and betacellulin [38], ADAM-10 has also been shown to function in the Notch signaling pathway.

Numerous reports have identified Kuzbanian (the ADAM-10 homologue in Drosophila) as being indispensable for Notch to function properly; for example Kuzbanian-deficient flies exhibit phenotypes related to Notch loss of function [39]. There are, however, conflicting reports implicating Kuzbanian as either an α-secretase responsible for cleaving the extracellular domain of Notch [40, 41], leading to Notch activation (Fig. 1), or as the protease responsible for cleaving Notch during its maturation [42], allowing for its expression on the cell surface (Fig. 2). With regards to the latter, it has been shown that Notch is initially expressed as a full-length monomer, but undergoes "S1" cleavage in the Golgi, producing a heterodimer, in order to be presented on the cell surface. The full-length Notch monomer is not present on the cell surface, and therefore cannot be activated [43], indicating that if Kuzbanian is indeed responsible for this essential S1 cleavage, Notch would not be able to function without intracellular Kuzbanian activity, regardless of other potential extracellular proteases available. While both the full-length and processed forms of Notch are detectable in wild type embryos, only the full-length form is detected in *kuzbanian*-null embryos [42], indicating that Kuzbanian controls proteolytic processing of Notch *in vivo*. Since most of the work done to identify ADAM-10's true role has been done in Drosophila using the homologue, Kuzbanian, and the lone Notch receptor present in Drosophila, its role in the more complex mammalian pathway has not been fully examined.

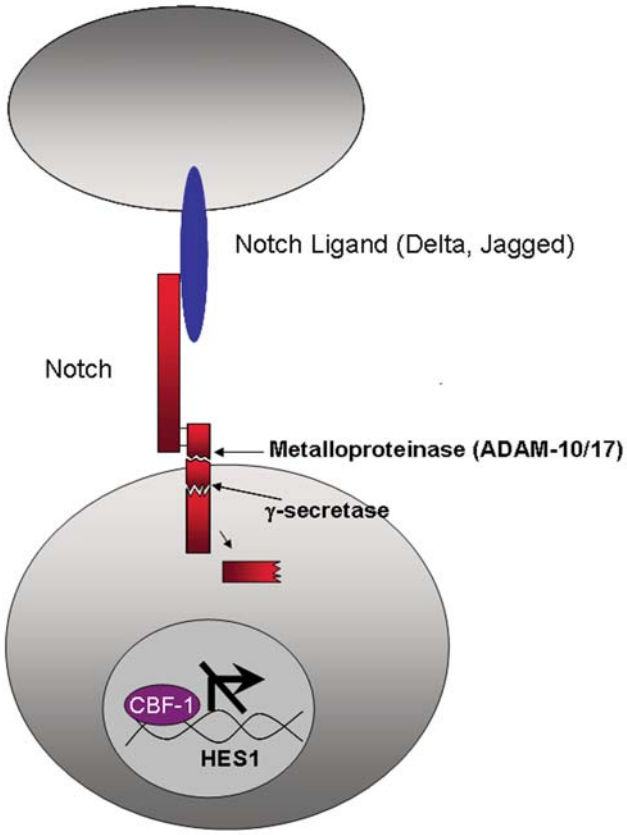

Figure Intro-1. Canonical Notch Signaling Pathway.

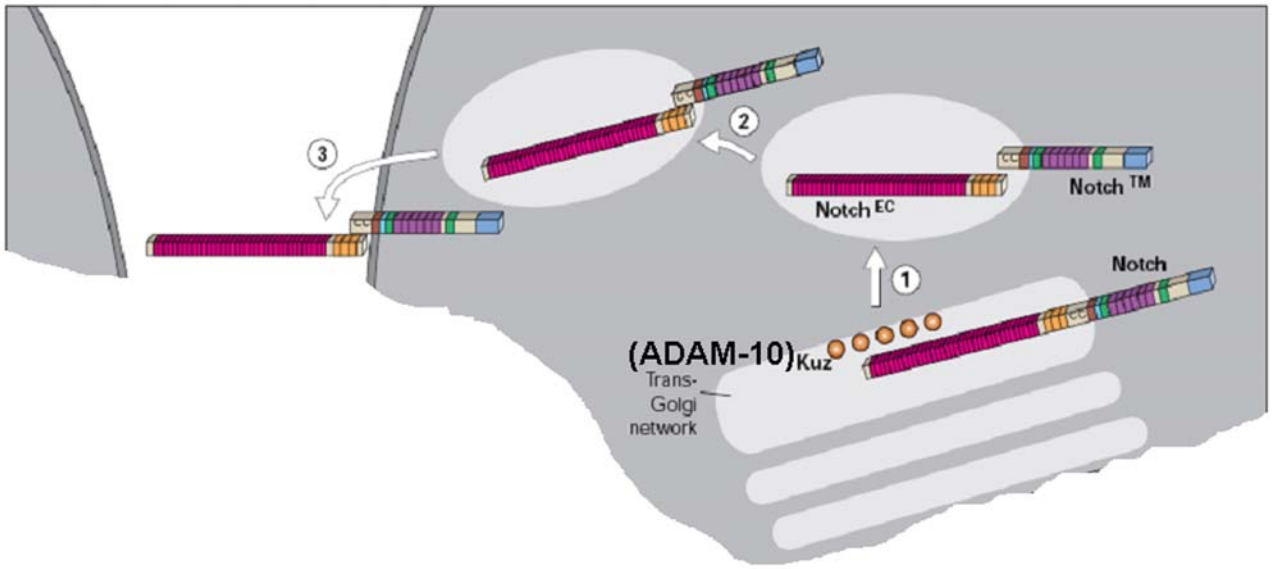

Figure Intro-2. Notch maturation and cell surface presentation. In Drosophila, Kuzbanian (ADAM-10-homologue) is required for intracellular Notch processing and subsequent presentation on the cell surface.

I. Matrix metalloproteinase 7 controls pancreatic acinar cell transdifferentiation by activating the Notch signaling pathway

Summary

Acinar-to-ductal metaplasia in the pancreas is associated with an increased risk for tumorigenesis. Molecular dissection of this process *in vitro* has shown that primary acinar cells, in response to EGF receptor ligands, can transdifferentiate into duct-like epithelia, passing through a nestin-positive intermediate, in a Notch pathway-dependent manner. Here, we have used the acinar cell explant model of ADM to test the direct contribution of MMP-7 to acinar transdifferentiation. We have determined that MMP-7 was expressed in response to TGF-α and that primary acinar cells derived from MMP-7$^{-/-}$ pancreata did not convert to duct cells. Experiments to determine the hierarchy of MMP-7 among other molecules that contribute to acinar transdifferentiation supported a model in which MMP-7 activity leads to Notch activation to induce the transition to the nestin-positive intermediate and thus for ADM. *In vitro* cleavage assays suggest MMP-7 may be able to cleave Notch directly, causing its activation.

Materials and Methods

Mice

The C57BL/6J MMP-7$^{-/-}$ mice were a gift from Lynn Matrisian (Vanderbilt University, Nashville, TN). Control C57BL/6J animals were purchased from The Jackson Laboratory. Animals were bred and maintained in a maximum isolation facility in the Division of Laboratory Animal Resources at Stony Brook University. All protocols herein were approved by the IACUC at Stony Brook University.

Primary Acinar Cell Cultures

Primary acinar cell cultures were prepared by modifying published protocols (Means). Pancreata were removed from 4- to 8-week-old male wild-type or matrix metalloproteinase type 7-null (MMP-7$^{-/-}$) mice and washed three times in ice-cold HBSS, spinning at 1000 rpm for 2 min in between washes. Pancreata were then minced with sterile scissors, spun down, the supernatant was removed, and acinar cells were digested in 0.2 mg/mL collagenase-P (Roche) rocking at 37ºC for 15 min. Digestion was stopped by adding ice-cold HBSS containing 5% FBS, the washing in same three more times. Collagenase-digested tissue was filtered through 500-µm and 105-µm polypropylene mesh (Spectrum Laboratories), in succession, then added drop-wise to HBSS containing 30% FBS. Filtrate was centrifuged through the HBSS/FBS at 2000 rpm for 2 min. The

pellet was resuspended in 1X Waymouth MB 752/1 medium (Sigma-Aldrich) supplemented with 100 μg/mL gentamicin, 1% FBS, 0.1 mg/mL soybean trypsin inhibitor (USB Corporation), and 1 μg/mL dexamethasone (Sigma-Aldrich). An equal volume of rat tail collagen type 1 (RTC) (BD Biosciences) (6 mL collagen, 600 μL 10X Waymouth, 400 μL 0.34 N NaOH) was added to the cellular suspension. The acinar cell/RTC mixture was divided into the wells of a 24-well plate and incubated at 37ºC, 5% CO_2 for 30 min to allow the collagen to solidify. Waymouth MB 752/1 medium (1X) supplemented with 1% FBS, and appropriate growth factors or inhibitors, was added. Transdifferentiation events were induced by addition of 50 ng/mL recombinant TGF-α (Chemicon International) or 200 ng/mL active rMMP-7 (Calbiochem) to medium. Where indicated, acinar cells were treated with 20 μM WPE III-31C (Calbiochem) in dimethyl sulfoxide. Cultures were maintained in a 37°C and 5% CO_2 incubator for 5 days with medium replaced on days 1 and 3.

Immunofluorescence

Antibodies used for immunofluorescence were as follows: mouse anti-nestin (BD PharMingen), rabbit anti-α-amylase (Sigma-Aldrich) or goat anti-α-amylase (Santa Cruz Biotechnology, Inc.), mouse anti-cytokeratin-19 (Novocastra Laboratories, Ltd.) or rabbit anti-cytokeratin (DAKO), rabbit anti-MMP-7 (Sigma-Aldrich), rabbit anti-GFP (Clontech), mouse anti-V5 (Invitrogen), rabbit anti-Notch-1 (6A5), and rabbit anti-cleaved Notch-1 (Val-1744) (Cell Signaling Technology). Immunofluorescent labeling of pancreatic explants was performed as described in ref. [19]. Collagen disks were removed from the 24-well plate and fixed in methanol/DMSO (4:1) overnight at 4ºC. Disks were stored in 100% methanol at -20ºC. Disks were rehydrated and washed with PBS. Cells were blocked with PBSMT (PBS + 0.5% Triton X-100 + 2% milk) for 2 h at room temperature and then incubated sequentially with the primary and secondary antibodies diluted in PBSMT overnight at 4ºC. Between antibody incubations, disks were washed in PBST. Disks were mounted using Vectashield containing DAPI (Vector Laboratories). For immunofluorescent labeling of COS-7 cells, cells were washed in ice-cold PBS and fixed in ice-cold methanol for 7 min. Cells were blocked in 3% milk/PBS 1 h at room temperature and incubated with primary antibody overnight at 4°C. After washing with PBS, secondary antibodies were added for 30 min at 37°C. Cells were washed with PBS and mounted with Vectashield + DAPI. Immunohistochemistry was carried out on formalin fixed, paraffin embedded tissue (gift of M. Kay Washington, Department of Pathology, Vanderbilt University) using previously described methods [26] with an antibody for Val1744 cleaved Notch-1 (Cell Signaling Technology). Immunofluorescence was performed with the same antibody using fresh pancreatic tissue harvested from 2-month old LSL$Kras^{G12D}$;p48Cre mice, frozen in OCT and sectioned. Secondary antibody was Alexa fluor 594-labeled anti-rabbit antibody (Invitrogen). Fluorescent images were captured on a Zeiss LSM-510 Meta confocal microscope and phase and GFP images on a Zeiss Axiovert 200M microscope.

Adenoviral Infections

Before embedding explants in collagen, 1 mL of cell suspension was placed in 35-mm bacterial Petri dishes. Adenoviruses encoding GFP, Notch-1-ICD, Notch-2-ICD, or dnRBP-Jκ [gifts from Lucy Liaw (Maine Medical Research Institute, Scarborough, ME) and Charles Eberhart (The Johns Hopkins University, Baltimore)] were added to the cell suspension at a multiplicity of infection (MOI) of 20:1. Cell/virus mixtures were rocked every 15 min for 1 h at 37°C and remained in suspension overnight. Suspensions were mixed with collagen in medium without growth factors.

Notch Cleavage in Intact Cells

COS-7 cells were cultured in DMEM + 10% FBS at 37°C in a humidified 95% air/5% CO_2 incubator. Cells (4×10^5) were transfected with 5 μg of pCDNA4V5-Notch-1 (gift from Deena Small, University of New Hampshire, Durham, NH) or a Notch-2 construct containing an extracellular 7Xmyc tag, with Lipofectamine 2000 (Invitrogen). Forty-eight hours later, the medium was replaced with OptiMEM (Invitrogen), containing 100 ng/mL pro-MMP-7 (Calbiochem), 0–200 ng/mL active rMMP-7 for 2–18 h, or 20 μM WPE III-31C, as indicated. In order to analyze the Notch extracellular domain in the medium, cells were treated with 200 ng/mL active recombinant MMP-7 (Calbiochem) or serum-free medium alone for 4 hours at 37°C. Medium was collected and spun at 18000 x g for 10 minutes in a microcentrifuge. The supernatant was analyzed by Western blotting using a myc antibody (Santa Cruz Biotechnology, Inc.). For EDTA activation, cells were washed in PBS and incubated in PBS + 10 mM EDTA for 15 min at 37°C. Cells recovered in DMEM for 4 h. For Western blotting, cells were washed in ice-cold PBS and lysed in ice-cold RIPA buffer (1% Nonidet P-40, 1% sodium deoxycholic acid, 0.1% SDS, 150 mM NaCl, 1 mM $NaHPO_4$, 0.2 mM EDTA, plus protease inhibitors). Twenty micrograms of lysate was resolved on a 5% SDS/polyacrylamide gel, transferred to nitrocellulose, blocked in 5% milk/TBST, and probed with primary antibody overnight at 4°C, followed by secondary antibody, and visualized by chemiluminescence.

***In Vitro* Notch Cleavage Assay**

A portion of the *notch-1* gene, encoding a fragment of the extracellular domain, was cloned into the pCAL-n vector (Stratagene). This vector tags the N-terminus of the protein with a calmodulin-binding peptide (CBP). Notch/CBP fusion protein was *in vitro* transcribed and translated in the presence of ^{35}S-methionine, using the T^NT Transcription/Translation System® (Promega), purified using calmodulin beads, and treated with 95 ng active recombinant MMP-7 or buffer alone for 1 hour at 37°C. Products were visualized by autoradiography.

RT-PCR Analysis

Total RNA was extracted using the RNeasy mini kit (Qiagen). cDNA was synthesized by using SuperScript II reverse transcriptase (Invitrogen), and PCR was carried out for targets with 25, 30, and 35 cycles to confirm linear range. The signal was normalized by

amplification of GAPDH for 22, 28, and 32 cycles. Primer sequences listed in Appendix 1.

Results

MMP-7 Is Necessary for Acinar Transdifferentiation. We have demonstrated that MMP-7 is necessary for most aspects of CP progression *in vivo*, including formation of MDLs [26]. However, the complexity of the *in vivo* model makes it difficult to determine how MMP-7 affects MDL formation. To test the hypothesis that MMP-7 directly controls ADM, we used a simplified *in vitro* system in which pancreatic tissue explants enriched in acinar, centroacinar, and associated terminal duct epithelium, and depleted of stromal and islet cells, are embedded in a three-dimensional collagen matrix and treated with TGF-α. The ensuing transdifferentiation, which passes through a nestin-positive intermediate [19], concludes with the appearance of a cytokeratin-19 (CK-19)-positive ductal phenotype within 5 days in culture [12].

To test the appropriateness of this system for assessing MMP-7 function in acinar transdifferentiation, we first determined whether MMP-7 was expressed under these culture conditions (Fig. 1). Acinar explants were prepared from pancreata of wild-type or MMP-7$^{-/-}$ mice, and the explants were embedded in collagen and treated with TGF-α under low-serum conditions. Duplicate cultures were fixed on consecutive days, and MMP-7 expression was determined by immunofluorescence, with MMP-7$^{-/-}$ explants as a negative control (Fig. 2). At day 0, MMP-7 was not detected, with strong expression found in 5.2% of acinar clusters on day 1, increasing to 54.5% on day 2, and to 69.7% on day 3 (Fig. 1). Expression of MMP-7 in these cultures was confirmed by semiquantitative RT-PCR (Fig. 2).

We then tested whether MMP-7 was necessary for acinar transdifferentiation. Wild-type and MMP-7$^{-/-}$ cultures were treated as before, fixed on day 5, and examined for the acinar and ductal markers amylase and CK-19, respectively, by coimmunofluorescence (Fig. 3). By day 5, wild-type explants developed an amylase-negative, CK-19-positive ductal phenotype in roughly 80% of cell clusters (Fig. 3A). In contrast, acinar cells from MMP-7$^{-/-}$ mice maintained a predominantly acinar phenotype in 85% of cell clusters, confirmed by the persistence of amylase and the absence of CK-19 expression throughout the culture period (Fig. 3B). To confirm that the block in transdifferentiation in MMP-7$^{-/-}$ cultures was the result of the immediate lack of MMP-7, we added active recombinant MMP-7 (rMMP-7) to the culture medium, which restored CK-19 positivity to 68% of MMP-7$^{-/-}$ cell clusters (Fig. 3C). We conclude that *in vitro* acinar transdifferentiation is highly dependent on MMP-7.

MMP-7 and Notch Are Required for Transition to the Nestin-Positive Intermediate. The Notch pathway has been shown to be responsible for maintaining stem and progenitor cell populations and blocks pancreatic acinar differentiation [15]. In acinar transdifferentiation, acquisition of the ductal phenotype is controlled by the Notch pathway [12]. To investigate whether Notch and MMP-7 functionally interact in this system, we set out to define where both act during the process. Initially, we examined the

effects of γ-secretase inhibition, which blocks intracellular Notch processing, on the transition to the nestin-positive intermediate. In wild-type acinar cells, nestin expression was discernable by immunofluorescence by day 3 (Fig. 4A), as reported [19]. In the presence of the γ-secretase inhibitor (GSI), WPE III-31C, nestin expression was not detected at day 3 (Fig. 4B) nor at any point in the 5 days of culture. Because the GSI can block the intramembrane cleavage of many proteins, we tested whether activating the Notch pathway could rescue nestin expression in the presence of the GSI. Indeed, infection with an adenovirus encoding the intracellular domain of Notch-1 (Ad-N1ICD), restored nestin positivity in the GSI-treated cultures (Fig. 4C), indicating that Notch is the relevant γ-secretase substrate in the assay. In parallel experiments, we found that MMP-$7^{-/-}$ acinar cells failed to initiate nestin expression at day 3 (Fig. 4D) or at any point during the 5-day culture period. Also, GSI treatment had no effect on MMP-7 expression itself (Fig. 5). Thus, activity of both Notch and MMP-7 was required for transition to the nestin-positive intermediate, and MMP-7 did not appear to be a downstream target of Notch.

Notch-ICD Bypasses the Requirement for MMP-7. Because Notch and MMP-7 appeared to be working in the same part of the transdifferentiation process, we set out to test whether they acted as components of the same pathway or independent essential pathways. To distinguish between these possibilities, we infected wild-type and MMP-$7^{-/-}$ acinar explants with Ad-N1ICD-V5 to induce transdifferentiation, instead of TGF-α, with a GFP-encoding adenovirus (Ad-GFP) as a negative control (Fig. 6). GFP and V5 immunofluorescence were used to confirm infection efficiency, consistently ≈90%. At 3 days after infection, cells were fixed and analyzed for CK-19 expression to test for acinar transdifferentiation. GFP controls showed negligible conversion to a ductal phenotype (Fig. 6C and I), whereas Ad-N1ICD-V5-infected cultures showed conversion of a majority of cells, approximately equivalent to the infection efficiency, in both wild-type and MMP-$7^{-/-}$ cultures (Fig. 6F&L). Thus, Notch activity bypassed the requirement for MMP-7, suggesting that Notch acts downstream of MMP-7 in a common pathway.

The ability of Notch to induce transdifferentiation in MMP-$7^{-/-}$ acinar cells suggested that MMP-7 acts upstream of Notch. To address this possibility directly, we tested whether MMP-7 was sufficient to induce Notch-dependent transdifferentiation. We performed the acinar transdifferentiation assay with wild-type acinar explants, replacing TGF-α with rMMP-7. Coimmunofluorescence for amylase and CK-19 showed that by day 5, MMP-7 induced the ductal phenotype (Fig. 7A). This process was blocked by GSI (Fig. 7B) as well as by infection with an adenovirus encoding a dominant-negative form of RBP-Jκ (Fig. 7C&D), which blocked CSL-dependent reporter activity (Fig. 8). Together, these data confirm that MMP-7 acts upstream of Notch to induce transdifferentiation.

MMP-7 Activates Notch. The most obvious model that fits the previous data is one where MMP-7 cleaves the extracellular domain of Notch, inducing subsequent γ-secretase intramembrane cleavage to form active Notch. To examine this possibility in detail, we moved to a system more amenable to biochemical analysis but with minimal background protease activity. We transfected COS-7 cells with a construct encoding full-

length Notch-1 with a C-terminal V5 tag (Notch-1-V5) and treated them with molar equivalent amounts of recombinant pro-MMP-7 or active MMP-7. To analyze Notch processing by immunoblot, we used an antibody (Cleaved N1 Val-1744) that is specific for the neoepitope of Notch-1 exposed after γ-secretase cleavage. Notch cleavage was induced only by active MMP-7 (Fig. 9A). As a control for antibody specificity, cells were treated with WPE III-31C along with active rMMP-7 (Fig. 9A), which eliminated the appearance of the neoepitope. In a time course, we found that γ-secretase-cleaved Notch-1 was evident 2 h after the addition of rMMP-7 (Fig. 9B). Titration of rMMP-7 showed that as little as 2 ng/mL enzyme induced γ-secretase processing of Notch-1, with optimal cleavage occurring with 20 ng/mL rMMP-7 (Fig. 9C). For independent confirmation of MMP-7-induced Notch processing, we performed immunoblots for the C-terminal V5 tag (Fig. 9D), which revealed a size shift in the overexpressed protein consistent with P2 and P3 site processing [44].

Continuing along the Notch pathway, we examined nuclear translocation of the Notch-ICD. COS-7 cells transfected with the full-length Notch-1-V5 expression vector were treated with medium alone or with medium containing active rMMP-7. After 4 h of treatment, cells were fixed and analyzed by coimmunofluorescence (Fig. 10A&B). V5 reactivity indicated transfected cells, and Cleaved N1 Val-1744 reactivity indicated Notch activation. With MMP-7 treatment, 34% of expressing cells exhibited cleaved nuclear Notch-1 compared with 10% of cells without MMP-7 (Fig. 10C).

Hes1, a Notch target gene, is often analyzed as an indication of Notch activity [12]. Using semiquantitative RT-PCR, we assayed for *hes1* transcript after MMP-7 treatment. COS-7 cells were transfected with Notch-1-V5 and treated with medium alone or medium containing active rMMP-7 for 4 h. EDTA-induced Notch activation was used as a positive control. Relative to medium alone, *hes1* was up-regulated 4.4-fold in response to rMMP-7 and 6.2-fold in response to EDTA (Fig. 10D). To analyze nuclear translocation of the Notch-ICD another way, we transfected COS-7 cells with a full-length Notch-1 construct containing a C-terminal, intracellular GFP tag. Cells were again treated for 4 h with rMMP-7, or medium alone. After treatment with rMMP-7, GFP was detected in the nuclei of living cells (Fig. 11A), but not in nuclei of cells treated with medium alone (Fig. 11B). Collectively, these data indicate that MMP-7 activity can lead to Notch-1 γ-secretase cleavage, nuclear translocation, and target gene expression.

MMP-7 Activates Notch in Acinar Cell Explants. With the observation that MMP-7 is necessary and sufficient to induce Notch-dependent acinar transdifferentiation and can induce Notch processing in COS-7 cells, we wanted to confirm that MMP-7 was required to activate endogenous Notch in acinar cells. First, we tested whether Notch-1 was expressed in wild-type and MMP-7$^{-/-}$ acinar cells by immunofluorescence and RT-PCR. We found that both wild-type and MMP-7$^{-/-}$ acinar explants expressed Notch-1 protein and transcript at day 0 (Fig. 12). Thus, neither TGF-α nor MMP-7 was required for Notch-1 expression. We then used Cleaved N1 Val-1744 immunofluorescence to determine the status of Notch-1 activation in these cells. Wild-type acinar cells exhibited cleaved Notch-1 by day 3 in the majority of clusters, whereas MMP-7$^{-/-}$ acinar cells did not show immunoreactivity at day 3 (Fig. 13A&B), or at any time during the assay. Cleaved Notch-1 immunofluorescence could be restored by including rMMP-7 in the

cultures (Fig. 13C). As a final confirmation of MMP-7-dependent Notch activation, we tested for the expression of Notch target genes *hes1* and *hey1* in the explants. We found that MMP-7$^{-/-}$ explants expressed 2.1- and 2.3-fold lower *hes1* and *hey1*, respectively, and that expression was restored when the cultures were supplemented with rMMP-7 (Fig. 13D). We conclude that MMP-7 is necessary for appropriate Notch processing and activation in primary acinar cells.

Discussion

Acinar-to-ductal metaplasia is strongly associated with pancreatic tumorigenesis [11, 45]. Previous studies have shown that metaplasia *in vivo* is marked by expression of Notch target genes and, *in vitro*, Notch signaling is both necessary and sufficient for acinar-to-ductal transdifferentiation [12]. Our previous *in vivo* studies have linked MMP-7 to the formation of MDLs in a duct obstruction model of CP [26]. In the current work, we have shown that MMP-7 is both necessary and sufficient for activation of Notch signaling in acinar cells, which leads to dedifferentiation to a nestin-positive intermediate that precedes acquisition of a ductal phenotype. Consistent with this result, we find that nestin expression and Notch cleavage temporally coincide (Fig. 14).

In this *in vitro* system, MMP-7 appears to function as a key mediator between TGF-α and Notch activation. MMP-7 expression requires TGF-α but not Notch activity. Notch-1 expression is constitutive, irrespective of TGF-α or MMP-7, but its cleavage by γ-secretase requires MMP-7. This cleavage appears to be extremely efficient, working with as little as 2 ng/mL rMMP-7. Dominant-active Notch-1 or Notch-2 can restore transdifferentiation in MMP-7$^{-/-}$ acinar cells, and MMP-7 can process both Notch-1 and Notch-2 (Fig. 15) to generate the active ICD domain that can travel to the nucleus and initiate target gene transcription.

The dependence of Notch activation on MMP-7 in this system is surprising. During development, Notch signaling typically works by Notch binding to its ligand on an adjacent cell, which induces the ligand-binding domain to be transendocytosed into the ligand-expressing cell [13]. This process exposes the transmembrane domain to cleavage by ADAM proteases [42, 44]. Interestingly, ligand-dependent proteinases are clearly present in COS-7 cells because overexpression of Jagged-1 induced robust activation of a CSL reporter construct in the absence of rMMP-7 (Fig. 16). Also, using a Notch-2 construct tagged on the extracellular domain (ECD), we found that the ligand-binding domain was not transendocytosed but released into the medium in the presence of rMMP-7 (Fig. 17). Finally, rMMP-7 can directly cleave peptides containing the P2 cleavage site of the extracellular domain of Notch-1 (Fig. 18). We hypothesize that overexpressed, secreted MMP-7, unlike membrane-bound ADAMs, can access the P2 cleavage site without ligand, albeit inefficiently, to cleave Notch. We generated a construct of Notch-1 containing an ELR→EVG mutation between the last LIN-12 repeat and the transmembrane domain. This mutation was made based on the MMP-7 cleavage site found in FasL [46]. When this peptide was incubated with rMMP-7, cleavage was still observed, possibly implying that when the preferential MMP-7 cleavage site is removed, MMP-7 can still cleave at a less-desirable second site, as is seen with FasL mutants. It is also possible that MMP-7 may act indirectly by activating ADAMs; however, ADAM

activation has been reported to occur intracellularly by a furin-like enzyme [47], making this possibility unlikely. Some preliminary data generated using murine embryonic fibroblasts (MEFs) obtained from conditional ADAM-10 and ADAM-17 knockout mice suggest that rMMP-7 is still able to activate Notch-2 when either of these enzymes are removed.

Despite the finding that Notch activation requires MMP-7 in this system, our data do not contradict what has been shown. We propose that Notch signaling in development is controlled by ligand-dependent cleavage by ADAMs. Consistent with this proposal, MMP-7$^{-/-}$ mice show no developmental defects attributable to impaired Notch activity, whereas ADAM-null mice do [48]. However, we postulate that in disease, Notch processing can follow an alternate activation mechanism induced by an abundance of MMP-7 and perhaps other proteases that are hyperexpressed in a given pathological condition. In this context, it is interesting that another *in vivo* disease model has been shown to depend on both Notch and MMP-7: intestinal tumor formation in *Apc*^{Min} mice. Blocking Notch activity with a GSI inhibits tumor progression in this system [21], whereas adenoma formation is suppressed in a MMP-7$^{-/-}$ background [27].

In conclusion, data from the current and previous studies [12] have supported a model in which Notch signaling is required for acinar cells to dedifferentiate and convert to MDLs. Recently, it has been shown that *K-ras*, the most commonly mutated oncogene in PDAC, requires tissue damage to induce PDAC when expression of the mutant *K-ras* is confined to adult acinar cells [49], lending support to the hypothesis that MDLs can act as preneoplastic lesions. Thus, Notch inhibition may prove useful in preventing pancreatic disease progression of both CP and PDAC. Previous studies would suggest that ADAM-specific inhibitors would be one way to prevent Notch activation, but our data suggest that broad-spectrum MMP inhibitors may be required to block this pathway fully in pancreatic disease.

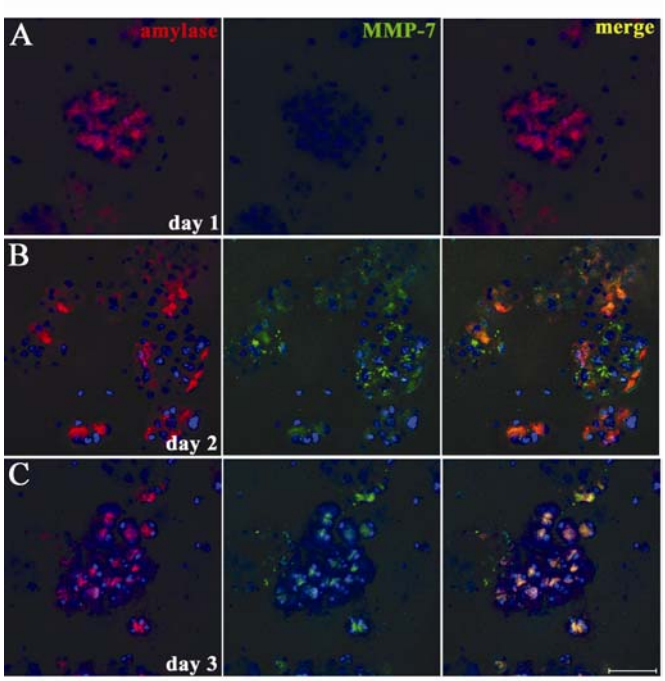

Figure I-1. MMP-7 is expressed in primary acinar cells treated with TGF-α. Pancreatic explants from wild-type mice embedded in collagen were treated with TGF-α. MMP-7 expression (green) was confirmed by immunofluorescence 1 (*A*), 2 (*B*), and 3 days (*C*) after culture, respectively. Staining was evident in the majority of acini on day 2. (Scale bar, 50 μm) Cells were costained for amylase (red) and DAPI (blue). Data are representative of five independent experiments.

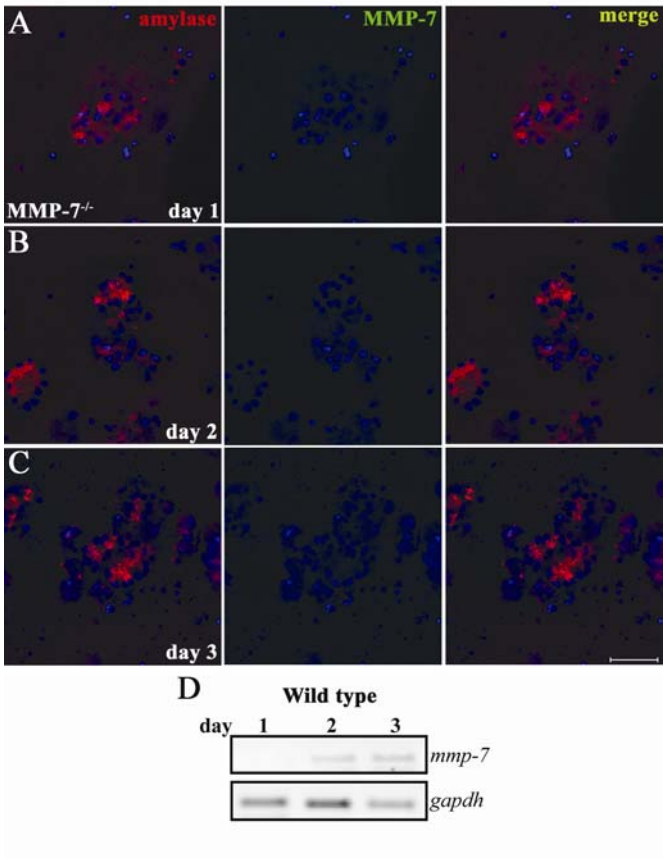

Figure I-2. MMP-7 immunoreactivity is absent in MMP-7$^{-/-}$ acinar cells, and MMP-7 RT-PCR confirms MMP-7 expression in wild-type acinar cells. (*A-C*) Primary acinar cells from MMP-7$^{-/-}$ mice embedded in collagen were treated with TGF-α. MMP-7 staining (green) was not found 1, 2, and 3 days after culture or on any day thereafter. (Scale bar, 50 μm) Cells were costained for amylase (red) and DAPI (blue). (*D*) RT-PCR for *mmp-7* in wild-type acinar cells treated with TGF-α showed *mmp-7* expression increased over the culture period.

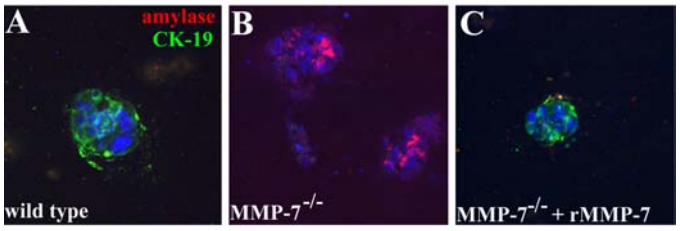

Figure I-3. MMP-7 is required for acinar-to-ductal transdifferentiation. Primary acinar cells from wild-type (*A*) and MMP-$7^{-/-}$ (*B&C*) mice were embedded in collagen and treated with TGF-α. Coimmunofluorescence for the acinar cell marker amylase (red) and the duct cell marker cytokeratin-19 (green) was performed on cells fixed on day 5. TGF-α treatment of wild-type cultures induced acinar-to-ductal transdifferentiation by day 5 (*A*). TGF-α treatment of MMP-$7^{-/-}$ acinar cells showed virtually no conversion to ductal structures (*B*). Addition of 200 ng/mL rMMP-7 with TGF-α to MMP-$7^{-/-}$ acinar cells (*C*) restored transdifferentiation. (Scale bar, 100 μm) DAPI is shown in blue. Data are representative of >10 independent experiments.

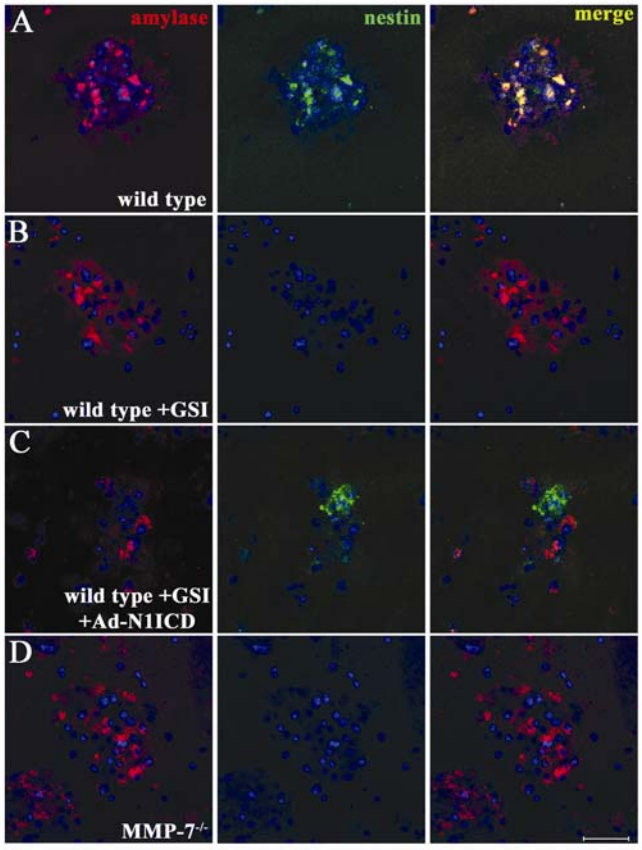

Figure I-4. Notch and MMP-7 are required for transition to the nestin-positive intermediate. Nestin immunofluorescence (green) was detectable on day 3 in wild-type cultures treated with DMSO (*A*), but not in cultures treated with 20 μM the γ-secretase inhibitor, WPE III-31C (GSI) (*B*). Infection with an adenovirus encoding a constitutively active V5-tagged Notch-1 intracellular domain (Ad-N1ICD-V5) bypassed the GSI, allowing nestin expression (*C*). Day 3 MMP-$7^{-/-}$ cultures did not show nestin immunoreactivity (*D*). (Scale bar, 50 μm) Shown are amylase in red and DAPI in blue. Data are representative of at least three independent experiments.

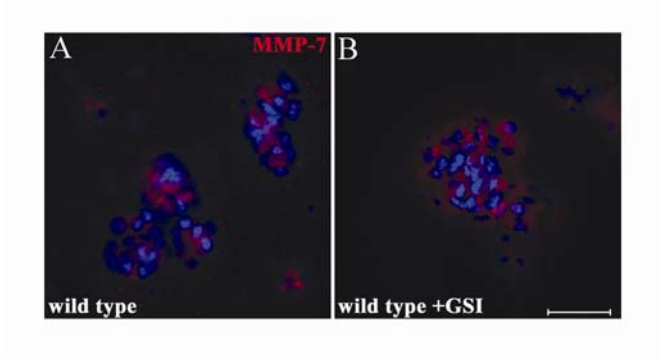

Figure I-5. Notch activity is not necessary for MMP-7 expression.
Immunofluorescence for MMP-7 was visible on day 2 in wild-type acinar cell cultures treated with TGF-α and either DMSO (*A*) or 20 μM γ-secretase inhibitor WPE III-31C (*B*). (Scale bar, 50 μm) DAPI is shown in blue.

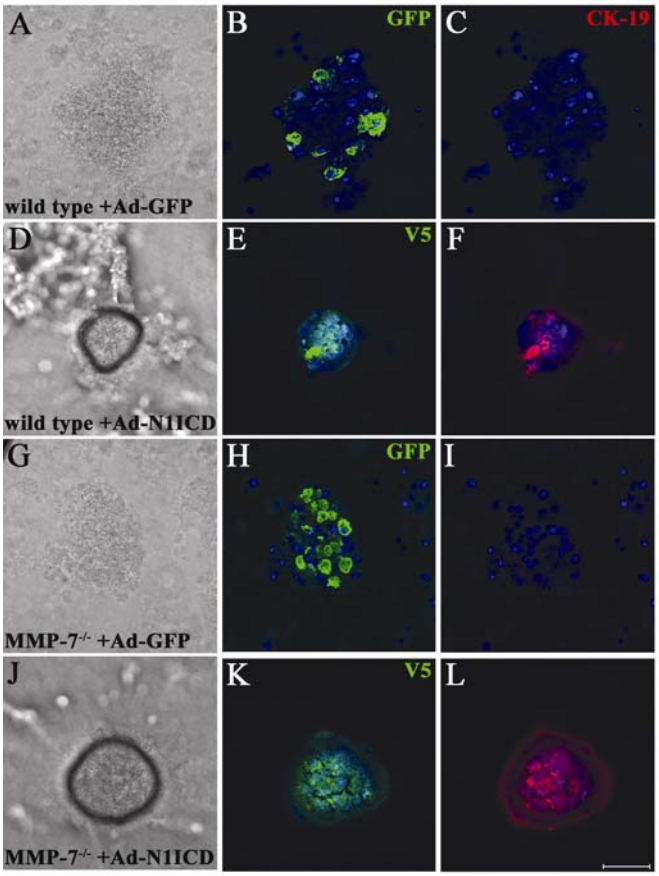

Figure I-6. Constitutively active Notch bypasses the requirement for MMP-7 in acinar transdifferentiation. Primary acinar cells from wild-type (*A–F*) or MMP-7$^{-/-}$ mice (*G–L*) were infected either with Ad-GFP, an adenovirus encoding GFP (*A–C* & *G–I*) or Ad-N1ICD-V5 (*D–F* & *J–L*) and embedded in collagen. After 3 days in culture, transdifferentiation in N1ICD cultures was evident (*D*&*J*) and was coincident with successful infection, confirmed by V5 immunofluorescence (*E*&*K*). Transdifferentiation was confirmed by immunofluorescence for CK-19 (*F*&*L*). (Scale bar, 50 μm) DAPI is shown in blue. Data are representative of three independent experiments.

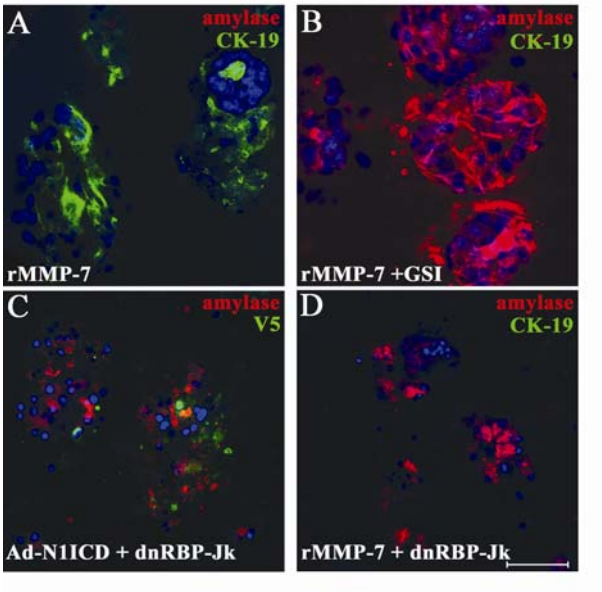

Figure I-7. MMP-7 activity is sufficient to induce Notch-dependent acinar-to-ductal transdifferentiation. (*A&B*) Primary acinar cells from wild-type mice were treated with 200 ng/mL rMMP-7 along with DMSO (*A*) or 20 μM WPE III-31C (GSI) (*B*). Coimmunofluorescence for amylase (red) and CK-19 (green) was performed on day 5. (*C&D*) Primary acinar cells infected with an adenovirus encoding a dominant-negative RBP-Jκ also blocked transdifferentiation induced by coinfection with Ad-N1ICD-V5 (amylase in red, V5 in green) (*C*) or by rMMP-7 (amylase in red, CK-19 in green) (*D*). (Scale bar, 50 μm) DAPI is shown in blue. Data are representative of at least three independent experiments.

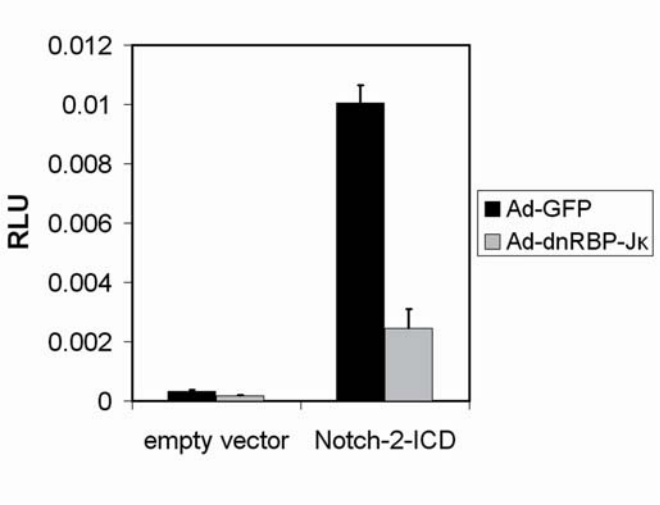

Figure I-8. Notch signaling is repressed by infection with an adenovirus encoding a dominant-negative RBP-Jκ. COS-7 cells were cotransfected with a CSL-driven luciferase reporter and either empty vector or Notch-2-ICD. Cells were infected with Ad-GFP or an adenovirus encoding dominant-negative RBP-Jκ (Ad-dnRBP-Jκ). Ad-dnRBP-Jκ repressed Notch activity by 4.1-fold.

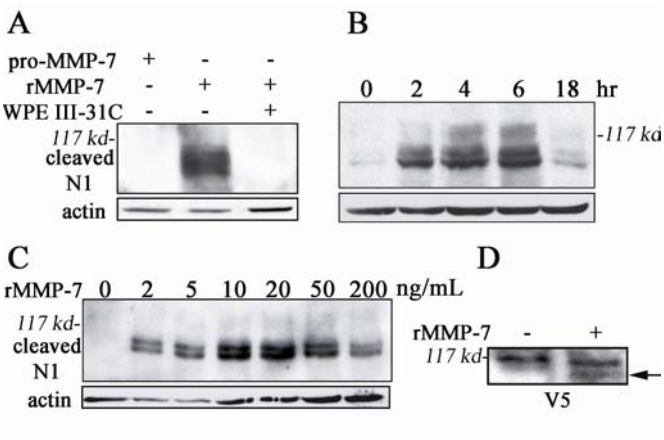

Figure I-9. MMP-7 activity induces γ-secretase cleavage of Notch-1. (*A–C*) Immunoblots for the γ-secretase-cleaved form of Notch-1 (Cleaved N1 Val-1744). (*A*) COS-7 cells expressing Notch-1 were treated with 100 ng/mL pro-MMP-7, 50 ng/mL active rMMP-7 with DMSO, or 20 μM WPE III-31C. (*B*) COS-7 cells expressing Notch-1 were treated with 200 ng/mL rMMP-7 for 0, 2, 4, 6, and 18 h. (*C*) COS-7 cells expressing Notch-1 were treated with varied rMMP-7 concentrations for 4 h. (*D*) COS-7 cells expressing Notch-1 with C-terminal V5 were treated with 200 ng/mL for 18 h. Data are representative of five independent experiments.

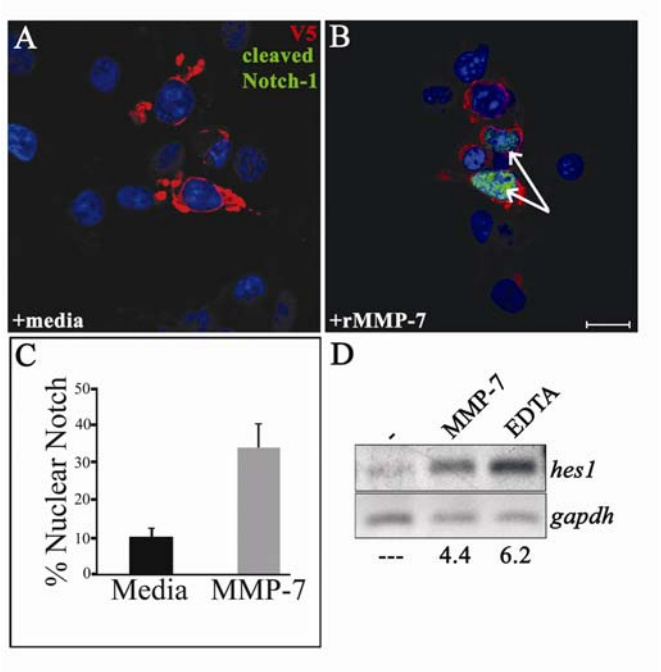

Figure I-10. MMP-7 activity leads to nuclear translocation of N1ICD and expression of *hes-1*. (*A&B*) COS-7 cells expressing full-length Notch-1 with a C-terminal V5 tag were treated for 4 h with MMP-7. Shown is immunofluorescence for Cleaved N1 Val-1744 antibody (green) and V5 antibody (red). (Scale bar, 20 μm) Cells were treated for 4 h with medium alone (*A*) or with rMMP-7 (*B*). Arrows indicate cells with nuclear cleaved Notch-1. DAPI is shown in blue. (*C*) Quantification of Notch-1 nuclear translocation. Percentage represents cells with nuclear Notch-1 divided by total cells expressing Notch-1. (*D*) RT-PCR for *hes1* from COS-7 cells expressing Notch-1 treated with MMP-7 or EDTA. Numbers represent fold expression relative to medium alone. Data are representative of five independent experiments.

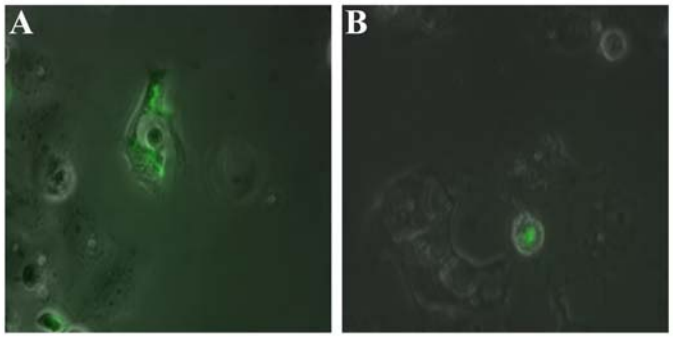

Figure I-11. MMP-7 activity leads to the nuclear translocation of N1ICD in living cells. (*A&B*) COS-7 cells expressing C-terminal GFP-tagged Notch-1 treated with medium alone (*A*) or rMMP-7 (*B*) for 4 h. Fluorescence was seen in the nuclei of living cells after rMMP-7 treatment (*B*).

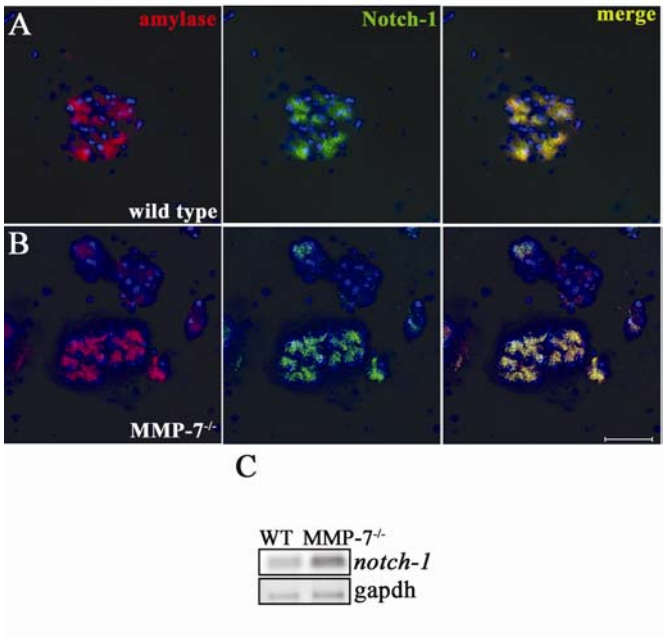

Figure I-12. Notch expression requires neither TGF-α nor MMP-7. Primary acinar cells from wild-type (*A*) and MMP-7$^{-/-}$ (*B*) mice were immunostained on day 0 for Notch-1 (green) and amylase (red). (Scale bar, 50 μm) Positive staining was independent of TGF-α or MMP-7 activity. DAPI is shown in blue. (*C*) Semiquantitative RT-PCR for *notch-1* from wild-type and MMP-7$^{-/-}$ acinar cells correlates with the immunofluorescence.

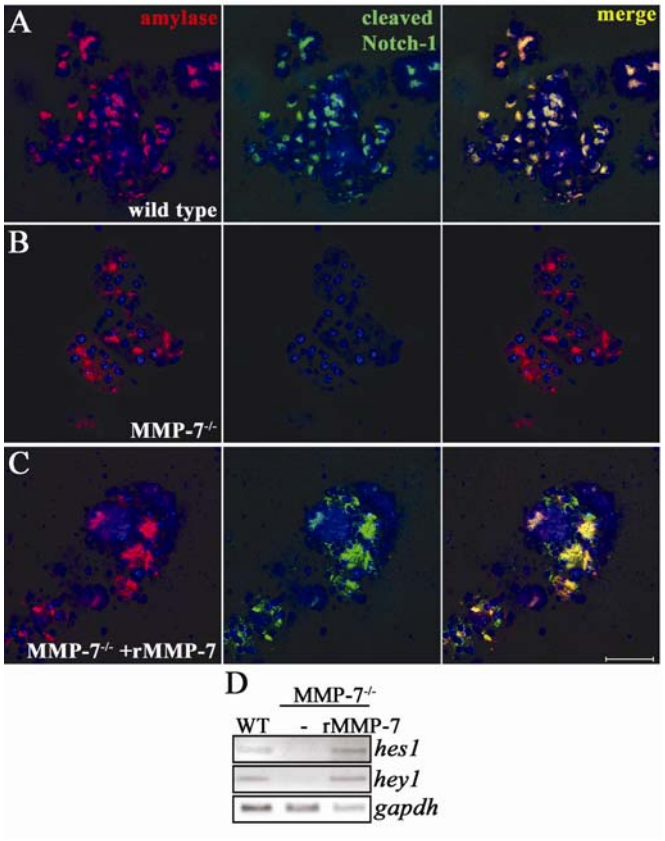

Figure I-13. MMP-7 is required for Notch activation in acinar explants. (*A–C*) Acinar explants immunostained for Cleaved N1 Val-1744 (green) and amylase (red) on day 3. Wild-type acinar cells exhibited Notch cleavage (*A*), whereas MMP-7$^{-/-}$ cells did not (*B*). Inclusion of 200 ng/mL rMMP-7 rescued Notch cleavage in MMP-7$^{-/-}$ acinar cells (*C*). (Scale bar, 50 μm) DAPI is shown in blue. (*D*) RT-PCR for *hes1* and *hey1* showed increased Notch activation in wild-type acinar cells and MMP-7$^{-/-}$ cells treated with rMMP-7, relative to MMP-7$^{-/-}$ cells. Data are representative of five independent experiments.

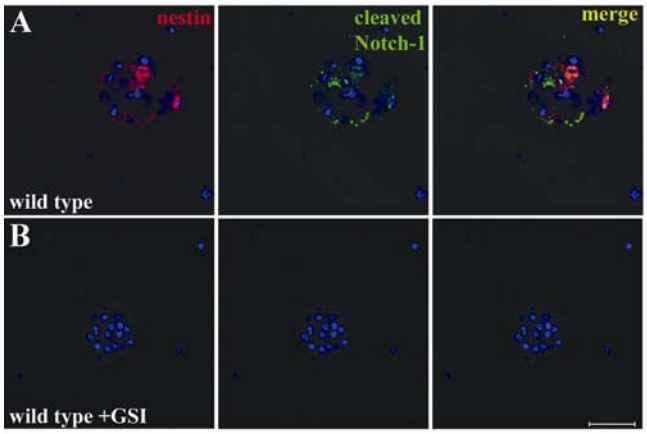

Figure I-14. Nestin expression and Notch activation coincide. Coimmunofluorescence for nestin (red) and Cleaved N1 Val-1744 (green) on day 3 in wild-type primary acinar cells. Cells treated with DMSO (*A*) showed evidence of nestin expression coincident with Notch cleavage, whereas cells treated with 20 μM γ-secretase inhibitor WPE III-31C (*B*) did not show either. (Scale bar, 50 μm) DAPI is shown in blue.

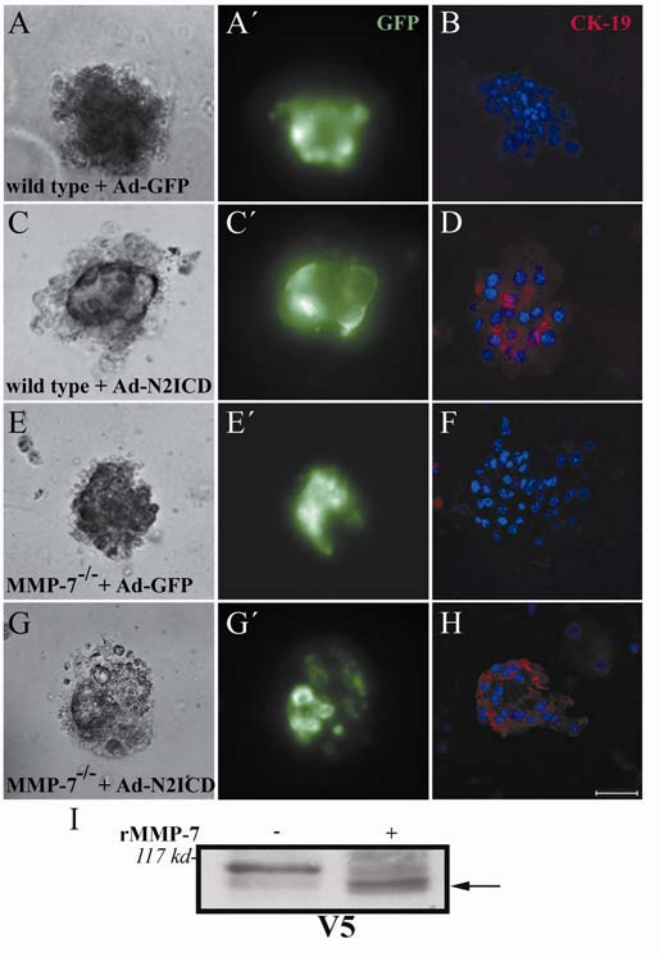

Figure I-15. Notch-2 behaves similarly to Notch-1 in that it can transdifferentiate MMP-7$^{-/-}$ acinar cells and is processed by rMMP-7. Primary acinar cells from wild type (*A*-*D*) or MMP-7$^{-/-}$ mice (*E*-*H*) were infected either with Ad-GFP, an adenovirus encoding GFP (*A*, *B*, *E* & *F*) or Ad-N2ICD, an adenovirus encoding the constitutively active Notch-2 intracellular domain and GFP (*C*, *D*, *G* & *H*) and embedded in collagen. After 3 days in culture, infection of acinar clusters, transdifferentiation in Ad-N2ICD cultures was evident by phase contrast microscopy (*A*, *C*, *E* & *G*) and was coincident with successful infection, confirmed by GFP fluorescence (*A′*, *C′*, *E′* & *G′*). Transdifferentiation was confirmed by immunofluorescence for CK-19 after fixation (*B*, *D*, *F* & *H*). (Scale bar, 100 μm) DAPI is shown in blue. (*I*) COS-7 cells expressing Notch-2 with C-terminal V5 treated with 200 ng/mL rMMP-7 for 18 h. Immunoblotting for the C-terminal V5 tag revealed that rMMP-7 induced a size shift consistent with P2 and P3 site processing of Notch-2.

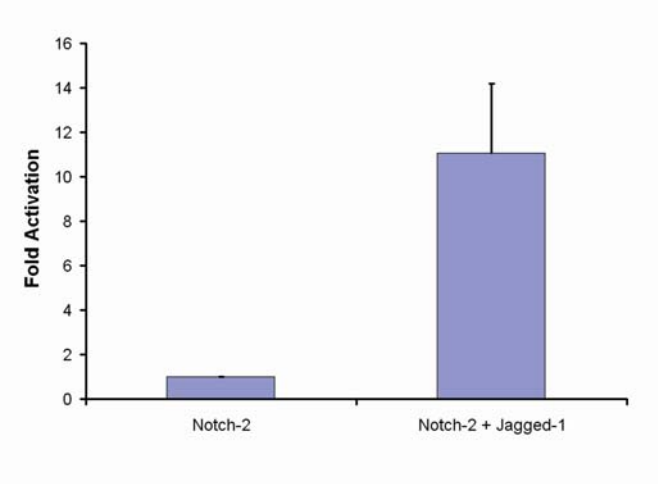

Figure I-16. Jagged-1 expression is sufficient to induce Notch activation in COS-7 Cells. COS-7 cells expressing a Notch-responsive artificial promoter and full-length Notch-2 were infected with Jagged-1 or control GFP adenovirus. Cells infected with Jagged-1 exhibited a roughly 11-fold induction of activity over cells infected with GFP.

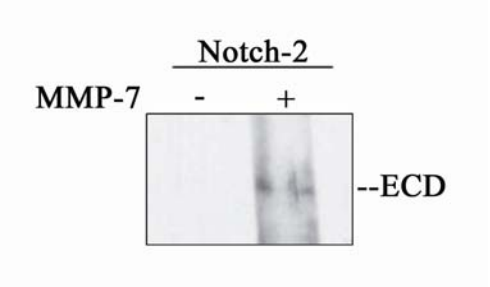

Figure I-17. The extracellular domain of Notch-2 is released upon MMP-7 treatment. COS-7 cells transfected with a Notch-2 construct containing an extracellular 7Xmyc tag were treated with active recombinant MMP-7 or serum-free medium alone. Using a myc antibody, the 220 kDa Notch-2-ECD was detected in the medium after MMP-7 treatment.

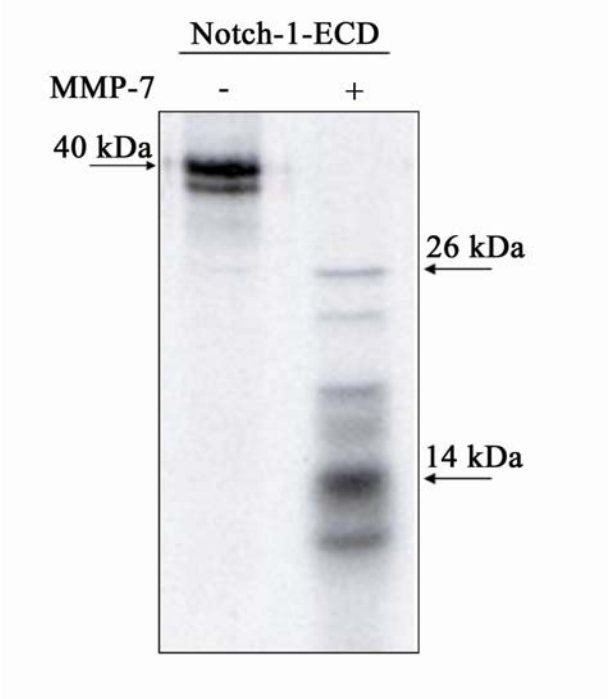

Figure I-18. MMP-7 directly cleaves Notch-1 *in vitro*. A peptide containing a region of Notch-1-ECD, including the metalloproteinase (P2) cleavage site, was treated with active recombinant MMP-7 or buffer alone. After MMP-7 treatment, among the fragments that appear are cleavage products of 26 and 14 kDa, consistent with a P2 site cleavage.

II. Conditional ablation of ADAM-10 extracellular protease activity results in defective Notch signaling

Summary

ADAM-10 knockout (ADAM-$10^{-/-}$) mice exhibit embryonic lethality, preventing analysis past that stage and into adulthood [48]. Shown here, we have generated a conditional ADAM-10 knockout mouse, allowing for tissue-specific removal of ADAM-10 and examination of ADAM-10's role beyond the full knockout's embryonic lethality. For initial characterization, we show that when recombination is ubiquitously induced by CMV-Cre, progeny die at embryonic day 9.5 (E9.5) and show signs of defective Notch signaling, phenocopying the ADAM-10-deficient embryos [48]. In addition, experiments using MEFs harvested from these mice support that the mechanism through which ADAM-10 is required for Notch activity is as an extracellular protease, not as an intracellular protease needed for Notch maturation and cell surface presentation. We further examine two tissues shown to require Notch activity for their functions, melanocytes and microglia, showing that the conditional knockout mouse is functional, and that the loss of ADAM-10 results in phenotypes associated with defective Notch signaling in these systems as well.

Materials and Methods

Generation and genotyping of conditional ADAM-10 knockout mice

The conditional ADAM-10 knockout mouse was engineered by Ingenious Targeting Laboratory, Inc. (Stony Brook, NY) in a C57BL/6J genetic background. The exon encoding for the zinc-binding region of ADAM-10, exon 9, was flanked by loxP sites and a *neo* cassette was introduced. The *neo* cassette was removed by crossing with a mouse expressing Flp1 (B6;SJL- Tg(ACTFLPe)9205Dym/J, backcrossed ten times to C57BL/6J) [50]. Primers used to detect floxed exon 9, yielding a 414 bp product for the floxed allele and a 235 bp product for the wild type allele, are in Appendix 1. Cre-mediated recombination was detected using primers upstream and downstream of the floxed alleles, yielding a 238 bp product after recombination and a 979 bp product without recombination, listed in Appendix 1. Primers used for Cre recombinase expression are listed in Appendix 1. DNA used for genotyping was extracted from either the tails of mice, or the heads of embryos. PCR conditions for genotyping were as follows: one cycle at 94°C for 5 minutes, thirty-five cycles of (94°C for 30 seconds, 55°C for 45 sec, 72°C for 45 sec), and one cycle at 72°C for 5 minutes.
ROSA26R *lacZ* reporter mice and CMV-Cre mice were purchased from Jackson Laboratories. The Tyr::$CreER^{T2}$ mouse was a gift from Marcus Bosenberg (University of

Vermont, Burlington, Vermont). All mice were bred and maintained in a maximum isolation facility in the Division of Laboratory Animal Resources at Stony Brook University. All protocols herein were approved by the IACUC at Stony Brook University.

Adenoviral infection and plasmid transfection

Cells were infected with Ad-GFP, Ad-Cre (gift from Dafna Dar-Sagi, New York University, New York, NY) or Ad-dnRBP-Jκ (gift from Lucy Liaw, Maine Medical Research Institute, Scarborough, ME) at a MOI of 20:1 in 25% of the final volume of complete DMEM, containing 10% FBS for the MEFs and 1% FBS for the microglia. Cell/virus mixtures were rocked every 15 minutes for 1 hour at 37°C, the remaining volume of media was added and cells were incubated at 37°C overnight. Cells were allowed to incubate for 48 hours prior to transfection, when applicable.
To enhance expression in MEFs, an adenovirus-mediated transfection procedure was used. Briefly, 1 μg pCDNA4V5-Notch-2 (gift from Deena Small, University of New Hampshire, Durham, NH) was incubated with Lipofectamine 2000 (Invitrogen) for 20 minutes in serum-free media at room temperature. Complete DMEM containing 10% FBS and appropriate adenovirus, at an MOI of 20:1, was then added to bring the volume up to 25% of the final volume. The infections were continued as described above.

MEF culture and luciferase

Murine embryonic fibroblasts were harvested from E12.5 embryos and maintained in complete DMEM medium containing 10% FBS. 48 hours after adenoviral infection, MEFs were transfected with 2 μg either empty pCDNA4V5 or pCDNA4V5-Notch-2, 1 μg 12XCSL-luc reporter plasmid (pGA981-6) [51] and 20 ng CMV-renilla (RL-CMV) control plasmid with Lipofectamine 2000. 24 hours after transfection, cells were lysed and luciferase activity was assayed using a luminometer. For rescue of ADAM-10 activity, cells were treated with 600 ng/mL active mouse recombinant ADAM-10 (Calbiochem) for 6 hours prior to lysis. All conditions were assayed in triplicate and statistical significance was evaluated by Paired Student's *t* test.

Primary microglia harvest and activation

Primary mixed cortical cell cultures were prepared from the brains of newborn ADAM-$10^{\text{flox-Ex9/flox-Ex9}}$ pups as described previously [52]. The mixed cortical cultures were used to isolate microglia after 11 days, when the cells were selectively released from the flasks by incubation with 15 mM lidocaine (Sigma-Aldrich) for 15 minutes at room temperature. After low-speed centrifugation, the cell pellet was resuspended in complete DMEM medium containing 1% FBS and plated onto poly-D-lysine-precoated 6-well plates. Primary microglial cells were activated with lipopolysaccharide (LPS) at 0.001 μg/mL for 6 hours.

Western blotting

Glycoproteins were concentrated in MEF and skin lysates by Concanavalin A (ConA) precipitation. Briefly, cells/tissues were lysed in RIPA buffer (1% Nonidet P-40, 1% sodium deoxycholic acid, 0.1% SDS, 150 mM NaCl, 1 mM $NaHPO_4$, 0.2 mM EDTA, plus protease inhibitors) and 600 μg lysate was diluted 1:1 with binding buffer (20mM Tris-Cl, pH 7.4, 0.5M NaCl). 40 μL packed ConA-sepharose beads (Calbiochem) were added and rocked 1.5 hours at room temperature. Beads were washed 3 times in binding buffer and protein was eluted in 50 μL sample buffer. Lysate was resolved on an 8% SDS/polyacrylamide gel, transferred to nitrocellulose, blocked in 5% milk/TBST, and probed with primary antibody overnight at 4°C, followed by secondary antibody, and visualized by chemiluminescence. Primary antibodies used were as follows: goat anti-ADAM-10 Ectodomain (R&D Systems), rabbit anti-V5 (Chemicon) and rabbit anti-actin (Sigma-Aldrich).

RT-PCR analysis

Total RNA was extracted using the RNeasy mini kit (Qiagen). Complementary DNA (cDNA) was synthesized by using SuperScript II reverse transcriptase (Invitrogen), and PCR was carried out for targets with 25, 30, and 35 cycles to confirm linear range. The signal was normalized by amplification of *gapdh* or *β-actin* for 22, 28, and 32 cycles. Primers sequences are listed in Appendix 1.

Tamoxifen induction

Tamoxifen (Sigma-Aldrich) was suspended in corn oil at a concentration of 10 mg/mL, and administered intraperitoneally (5 mg/40 g body mass) on postnatal (P) days 28, 29 and 30. Mice were sacrificed on P42, the skin was harvested and either lysed in RIPA buffer for analysis by Western blotting, lysed and homogenized (according to Qiagen instructions) for analysis by RT-PCR, or paraffin-embedded after X-gal staining.

X-gal staining

X-gal staining was carried out as previously described [53]. Briefly, tissues were rinsed in cold PBS and fixed in PBS containing 0.25% glutaraldehyde for 40 minutes at 4°C. The tissues were rinsed in PBS, incubated twice, for 20 minutes each, in permeabilization solution (2 mM MgCl2, 0.01% sodium deoxycholate, 0.02% NP-40), and stained by incubation in X-gal buffer (0.4 mg/mL 5-bromo-4-chloro-3-indolyl-D-galactoside, 2 mM potassium ferricyanide, 2 mM potassium ferrocyanide, and 4 mM MgCl2, 0.01% sodium deoxycholate, 0.02% NP-40 in PBS) for 48 hours at 30°C. Staining was stopped by incubating the tissues for 3 hours in PBS containing 4% paraformaldehyde, skin was washed by incubation in PBS overnight at 4°C, and embedded in paraffin by standard methods.

Cell surface biotinylation

48 hours after MEFs were infected with adenovirus, they were transfected with pCDNA4V5-Notch-2 for 24 hours. Cells were washed three times in ice-cold PBS, and then incubated with 2 mM EZ-link sulfo-NHS-Biotin (Pierce), or with ice-cold PBS (control), for 20 minutes at 4°C. The biotinylation reagent was then removed, and cells were washed twice and incubated once with ice-cold 100 mM Tris-HCl (pH 8.0) for 15 minutes. Cells were lysed in 300 µL RIPA buffer and cleared by centrifugation. Avidin-agarose (50 µL) (Pierce) was added to 600 µL of lysate and incubated overnight at 4°C. The avidin-agarose was pelleted by brief centrifugation, the lysate was removed and avidin-agarose was washed five times with RIPA buffer, and then resuspended in 75 µL sample buffer.

Results

Conditional Disruption of *adam-10* in Mice. In order to create a conditional knockout of ADAM-10, we used the Cre/loxP site-specific recombination system [54] to disrupt *adam-10* gene transcript. We flanked exon 9, encoding for the zinc-binding domain of ADAM-10, with loxP sites and a *neo* cassette was introduced by homologous recombination (Fig. 1A). Upon Cre recombination, exon 9 is deleted which causes downstream sequence to be out of frame, resulting in nonsense transcript beyond that point. The *neo* cassette was removed through breeding with a Flp1 recombinase-expressing mouse. Genotyping for the floxed allele, using primer set P2/P3, confirms the generation of wild type, heterozygous and homozygous floxed mice (Fig. 1B), all of which are viable and fertile.

To characterize Cre-induced recombination, homozygous floxed *adam-10* (ADAM-$10^{\text{flox-Ex9/flox-Ex9}}$) MEFs were harvested and infected with an adenovirus encoding either Cre recombinase (Ad-Cre) or GFP (Ad-GFP). MEFs infected with Ad-Cre did not express full length *adam-10* transcript (Fig. 2A) or messenger RNA (mRNA) (Fig. 2B) 48 hours after infection. In addition, we showed that neither *adam-9* nor *adam-17* levels are changed when ADAM-10 is removed (Fig. 2B), showing there is no compensatory increase of these other major ADAMs in these cells. Western blotting (Fig. 2C) using an ectodomain-specific antibody confirmed the loss of ADAM-10 precursor protein.

ADAM-$10^{\text{flox-Ex9/flox-Ex9}}$;CMV-Cre Mice Phenocopy ADAM-$10^{-/-}$ Mice. ADAM-10-deficient embryos are two-thirds the size of their littermates at day E9.5, and show notochord defects [48]. In order to test if the conditional ADAM-10 knockout mouse can phenocopy the ADAM-$10^{-/-}$ mouse, we crossed the ADAM-$10^{\text{flox-Ex9/flox-Ex9}}$ mouse with a transgenic mouse expressing Cre driven by the cytomegalovirus (CMV-Cre) promoter, which is ubiquitously expressed, to produce a complete ADAM-10 knockout mouse [55]. On E9.5, ADAM-$10^{\text{flox-Ex9/flox-Ex9}}$;CMV-Cre mice were less than two-thirds the size of their littermates, heterozygotes with CMV-Cre and mice lacking CMV-Cre (Fig. 3A&B). No ADAM-$10^{\text{flox-Ex9/flox-Ex9}}$;CMV-Cre pups, out of at least five litters, survived to term. ADAM-$10^{\text{flox-Ex9/flox-Ex9}}$;CMV-Cre embryos also exhibited defects in somitogenesis, as seen in ADAM-10-deficient embryos [48], illustrated by a fused region of somites, whereas in wild type embryos, the notochord was phenotypically normal (Fig. 3C&D).

To further confirm the phenotype observed in the complete ADAM-10 knockout mice, we examined Notch pathway components in ADAM-10$^{flox\text{-}Ex9/flox\text{-}Ex9}$ MEFs infected with Ad-Cre or Ad-GFP. Semiquantitative RT-PCR confirmed that expression of a downstream target gene of Notch signaling, *hes5*, was decreased after Cre recombination compared to Ad-GFP-infected MEFs, however, *notch-1* levels were not changed when ADAM-10 is lost (Fig. 3E). This mimics the Notch pathway-defective phenotype displayed in the ADAM-10$^{-/-}$ mouse [48].

ADAM-10 α–secretase Activity is Required for Proper Notch Activity. In order to identify the mechanism through which the loss of ADAM-10 results in defective Notch signaling, we examined Notch activity quantitatively using a luciferase assay. ADAM-10$^{flox\text{-}Ex9/flox\text{-}Ex9}$ MEFs were infected with Ad-Cre or Ad-GFP. 48 hours after infection, cells were transfected with either full-length Notch-2 or empty vector and a Notch-responsive artificial promoter, containing twelve CSL binding sites, cloned upstream of a luciferase reporter [51]. Luciferase activity was analyzed 24 hours post-transfection. ADAM-10$^{flox\text{-}Ex9/flox\text{-}Ex9}$ MEFs infected with Ad-GFP and expressing full-length Notch-2 exhibited a 2.2-fold increase in CSL-luciferase compared to cells infected with Ad-GFP and transfected with empty vector (Fig. 4). Conversely, ADAM-10$^{flox\text{-}Ex9/flox\text{-}Ex9}$ MEFs infected with Ad-Cre and expressing Notch-2 did not activate CSL-luciferase over the basal, empty vector-transfected level, indicating a requirement of ADAM-10 for Notch activation and CSL-dependent transcription. To ensure that the perturbation of Notch activity seen was not due to an arbitrary effect of Cre itself, we infected wild type MEFs with Ad-Cre and observed no effect on Notch activity, as compared to Ad-GFP-infected wild type MEFs. Treating the cells for 6 hours with a cell-impermeable active form of the ADAM-10 ectodomain restored Notch activity in the Cre-infected MEFs (Fig. 4). This result indicated that the downregulation of Notch activity seen in the Ad-Cre-infected MEFs is due to the lack of ADAM-10, and that ADAM-10 is capable of acting as an extracellular protease that can activate Notch signaling.

ADAM-10 Activity is Not Required for Cell Surface Presentation of Notch. Next, we explored ADAM-10's other putative role in the Notch signaling pathway: cleaving Notch intracellulary to allow the Notch heterodimer to be presented on the cell surface. In order to examine this, we again used ADAM-10$^{flox\text{-}Ex9/flox\text{-}Ex9}$ MEFs infected with Ad-Cre or Ad-GFP. 48 hours post-infection, the cells were transfected with an expression construct encoding full-length Notch-2 containing a C-terminal, intracellular V5 tag (Notch-2-V5). 24 hours post-transfection, cell surface biotinylation was performed, followed by streptavidin precipitation. ADAM-10$^{flox\text{-}Ex9/flox\text{-}Ex9}$ MEFs either infected with Ad-GFP or Ad-Cre showed Notch-2 expression on the cell surface, indicating proper intracellular processing (Fig. 5A). Input lanes showed expression of Notch-2-V5 in both sets of infected MEFs. To demonstrate that intracellular protein was not being biotinylated, controls with a cytoplasmic protein (β-actin) were performed with each sample. In order to verify that S1 cleavage is not affected, we analyzed lysates from the infected MEFs expressing Notch-2-V5 for Notch-2 processing by Western blotting. S1-processing of Notch-2-V5 in cells not expressing ADAM-10 was similar to ADAM-

10 containing cells (Fig. 5B). Thus, the loss of ADAM-10 does not affect S1 processing or cell-surface expression of the Notch protein in these cells.

Conditional Loss of ADAM-10 in the Skin Results in Defective Notch Signaling. To further characterize the conditional ADAM-10 knockout mouse, we wanted to ensure that Cre recombination resulted in the loss of ADAM-10 *in vivo*, using a system where Notch has been shown to be active. First, to establish our system, we crossed ROSA26R *lacZ* reporter mice [56] with mice expressing a tamoxifen-inducible, estrogen receptor-fused Cre recombinase under the control of the tyrosinase promoter (Tyr::CreER^{T2}). The Tyr::CreER^{T2} mouse efficiently induces Cre recombination in melanoblasts specifically after tamoxifen induction [57]. Twelve days after treatment with tamoxifen, the ROSA26R;Tyr::CreER^{T2} mice were sacrificed and their skin was harvested and stained with X-Gal, showing positivity in melanocytes, as expected (Fig. 6). Mice treated with corn oil alone did not show X-gal positivity (Fig. 6).

Recently, Notch signaling has been shown to be essential for the survival of melanocyte stem cells, and consequently, for proper hair pigmentation. We generated ADAM-10$^{flox\text{-}Ex9/flox\text{-}Ex9}$ mice expressing the Tyr::CreER^{T2} transgene (ADAM-10$^{flox\text{-}Ex9/flox\text{-}Ex9}$;Tyr::CreER^{T2}). Twelve days after tamoxifen treatment, recombination was assayed by PCR and showed the recombined allele specifically in the skin of ADAM-10$^{flox\text{-}Ex9/flox\text{-}Ex9}$;Tyr::CreER^{T2} mice treated with tamoxifen, while the nonrecombined floxed allele was detected in ADAM-10$^{flox\text{-}Ex9/flox\text{-}Ex9}$ mice without Cre (Fig. 7A). Using semiquantitative RT-PCR and Western blotting, we confirmed the loss of *adam*-10 mRNA and protein, respectively, in tamoxifen-treated ADAM-10$^{flox\text{-}Ex9/flox\text{-}Ex9}$;Tyr::CreER^{T2} skin, compared to ADAM-10$^{flox\text{-}Ex9/flox\text{-}Ex9}$ skin (Fig. 7B&C). In addition, using semiquantitative RT-PCR, we observed that the loss of ADAM-10 in the skin resulted in defects in Notch signaling, exhibited by decreased *hes1* expression, and an unexpected increase in *hey1* expression (Fig. 7B).

Loss of ADAM-10 Phenocopies Notch-1 Knockdown in Microglia. Recently it has been reported that Notch helps to maintain microglial cells in a quiescent state under normal conditions, and inhibits over-activation during pro-inflammatory events [58]. In order to determine if the loss of ADAM-10 can mimic the loss of Notch signaling in microglia, we harvested primary microglial cells from ADAM-10$^{flox\text{-}Ex9/flox\text{-}Ex9}$ mice and infected them with Ad-Cre or Ad-GFP. 48 hours post-infection, microglial cells were activated by incubation with LPS for 6 hours, and total RNA was extracted. Microglia infected with Ad-Cre effectively lost full length *adam-10* transcript, compared to cells infected with GFP, as determined by semiquantitative RT-PCR (Fig. 8A). In activated ADAM-10$^{flox\text{-}Ex9/flox\text{-}Ex9}$ microglial cells infected with Ad-Cre, *interleukin-6* (*il-6*) was increased roughly 26-fold, and *tnf-*α roughly 9-fold over LPS-treated ADAM-10$^{flox\text{-}Ex9/flox\text{-}Ex9}$ microglial cells infected with Ad-GFP, similar to the relationship shown when *notch-1* transcript is knocked down by RNAi (Fig. 8B-D) [58]. To further determine if the increase in cytokine levels was due to defective Notch signaling, we infected ADAM-10$^{flox\text{-}Ex9/flox\text{-}Ex9}$ microglial cells with an adenovirus encoding a dominant-negative RBP-Jκ (Ad-dnRBP- Jκ), which was demonstrated previously to block downstream Notch signaling (see previous chapter). After LPS activation, ADAM-10$^{flox\text{-}Ex9/flox\text{-}Ex9}$ microglial

cells infected with Ad-dnRBP-Jκ exhibited a roughly 71- and 10-fold in *il-6* and *tnf-α*, respectively, over activated ADAM-10$^{flox\text{-}Ex9/flox\text{-}Ex9}$ microglial cells infected with Ad-GFP (Fig. 8B-D). These results confirm that impaired Notch signaling leads to increased cytokine expression during microglial activation, and that the loss of ADAM-10 can phenocopy this observation.

Discussion

Herein, we have introduced a viable, fertile and functional conditional ADAM-10 knockout mouse. When recombination was ubiquitous, this mouse phenocopied the ADAM-10$^{-/-}$ mouse, showing lethality at day E9.5, and defective Notch signaling. In addition, we have shown that tissue-specific Cre recombination, and subsequent ADAM-10 loss, is efficient using this model. We have also provided evidence that ADAM-10's role in the Notch signaling pathway is as an α-secretase, required for the extracellular processing of Notch, not as a protease required for Notch maturation and presentation on the cell surface, as is Kuzbanian in Drosophila.

Previously, the ADAM-10$^{-/-}$ mouse allowed analysis only up to E9.5 [48]. With this conditional ADAM-10 knockout model, we have been able to analyze two tissue systems, the skin and brain, not previously possible in postpartum mice. We show that loss of ADAM-10 specifically in the skin results in defects in Notch signaling, exhibited by decreased *hes1* expression. We were surprised to find that ADAM-10 was not detectable in the skin after melanocyte-specific removal, at both the transcript and protein level. This efficient removal may indicate that ADAM-10 expression in the skin is normally restricted to melanocytes. It has been reported that when both Notch-1 and Notch-2, or RBP-Jκ alone, are conditionally removed using tyrosinase-driven Cre recombinase, hair pigmentation is lost, resulting in mice with a gray coat [59, 60]. Surprisingly, when ADAM-10 was removed in a similar manner, using a tamoxifen-inducible system, we did not observe this loss of pigmentation, even after approximately six hair cycles. One explanation for this may be that other ADAMs compensate for ADAM-10 in this system. Perhaps different ADAMs are required at different stages of development, as implicated by the fact that ADAM-10 knockouts die at E9.5, while ADAM-17 knockouts display peri-natal lethality and some animals can survive beyond weaning [61], and then during adulthood they can compensate for each other, maybe simply by their co-expression. We show here neither ADAM-9 nor ADAM-17 expression is upregulated in response to losing ADAM-10 in MEFs. Another possible explanation arises with the observation that *hey1* expression is upregulated, both in MEFs and skin, when ADAM-10 is removed, indicating that perhaps Notch activity is not fully impaired in this system. When we assayed for CSL-dependent Notch activity, we saw a definitive loss of luciferase activity, which contradicts the increase in *hey1*. Taking these results into account, Notch downstream targets appear to be differentially regulated, with some being independent of RBP-Jκ, as examined previously [62, 63].

In all cases presented here, we show defects in Notch signaling when ADAM-10 is removed. In embryos lacking ADAM-10, the defective somitogenesis is similar to that seen in Presenilin1/Presenilin2 double knockout mice [64]. In skin lacking ADAM-10,

we show that expression of a downstream target of Notch, *hes1*, is disturbed. Finally, activated microglial cells lacking ADAM-10 exhibit increased transcription of pro-inflammatory cytokines similar to that seen when *notch-1* transcript is decreased [58]. We offer here clear and distinct contexts in which ADAM-10 is required for Notch activity.

Others have shown a role of ADAM-10 in Notch signaling, but it still remains controversial over what exactly that role is. There is evidence that suggests ADAM-10/Kuzbanian is necessary for proper Notch maturation [42], as well as being responsible for the extracellular cleavage of Notch [40, 41]. Here, we show that ADAM-10 clearly has an extracellular role in activating Notch. The possibilities remain that ADAM-10 may be cleaving Notch directly, as shown in Drosophila [41], or that it is required to activate other proteases, such as ADAM-17, which in turn activate Notch. Increasing evidence suggests that different proteases may be responsible for the extracellular cleavage in a tissue-specific manner. Another possibility is that ADAM-10's major role is to cleave the Notch ligand, Delta-1 [65], releasing its extracellular domain, possibly leading to increased Notch activity. Either way, we have at least ruled out one possibility in our system. ADAM-10 is not required for Notch to be processed properly during its maturation, or to make it to the cell surface. Although this hypothesis has been reasoned based upon data obtained in Drosophila, we believe we have shown this not to be the case in a mammalian context.

In summary, we introduce here the conditional ADAM-10 knockout mouse. We provide evidence that recombination leads to the loss of ADAM-10 protein in a tissue-specific manner. We confirm that extracellular ADAM-10 protease activity is important for proper Notch signaling, and that depending on the specific tissue, there may be compensation for ADAM-10 loss.

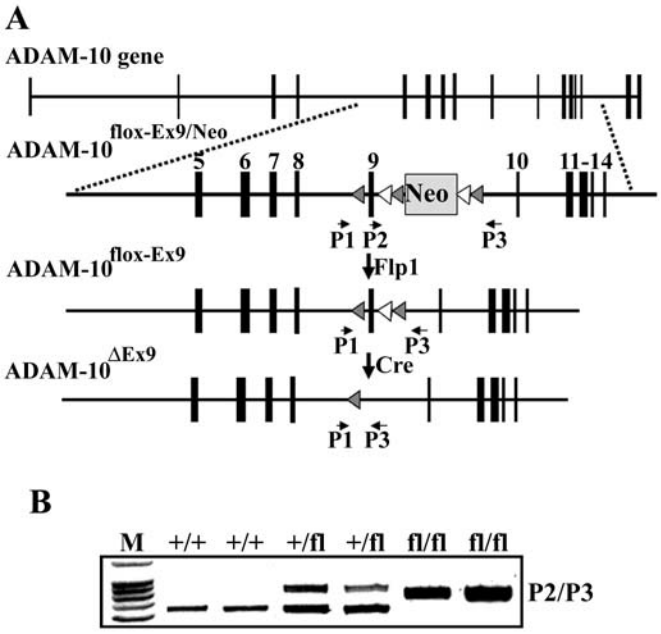

Figure II-1. Description of conditional ADAM-10 knockout. (*A*) Description of *adam-10* gene showing exon 9 flanked by loxP sites (shaded arrows), placement of the *neo* cassette and surrounding Flp1 recombinase targets (white arrows), and primer annealing sites. Upon Cre recombination, exon 9 will be removed, resulting in nonsense transcript beyond that point. (*B*) Genotyping using primer set P2/P3 confirms the generation of wild type (+/+), heterozygous (+/fl) and homozygous (fl/fl) floxed mice.

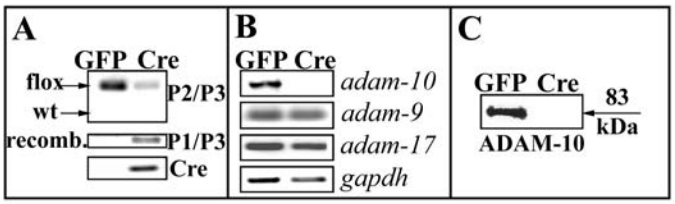

Figure II-2. Confirmation of conditional ADAM10 knockout. (*A*) Genotyping of ADAM10$^{flox\text{-}Ex9/flox\text{-}Ex9}$ MEFs infected with either Ad-GFP or Ad-Cre. Primer set P2/P3 is used to identify the floxed allele, while P1/P3 is used to confirm Cre recombination. A 238 bp product from P1/P3 indicates Cre-mediated recombination. (*B*) Semiquantitative RT-PCR showing translation of *adam10* is lost in ADAM10$^{flox\text{-}Ex9/flox\text{-}Ex9}$ MEFs infected with Ad-Cre, and no compensation is made by *adam9* or *adam17* in ADAM10$^{flox\text{-}Ex9/flox\text{-}Ex9}$ MEFs infected with Ad-Cre. (*C*) Western blotting confirms the loss of ADAM10 protein in ADAM10$^{flox\text{-}Ex9/flox\text{-}Ex9}$ MEFs infected with Ad-Cre. Results were confirmed over multiple experiments.

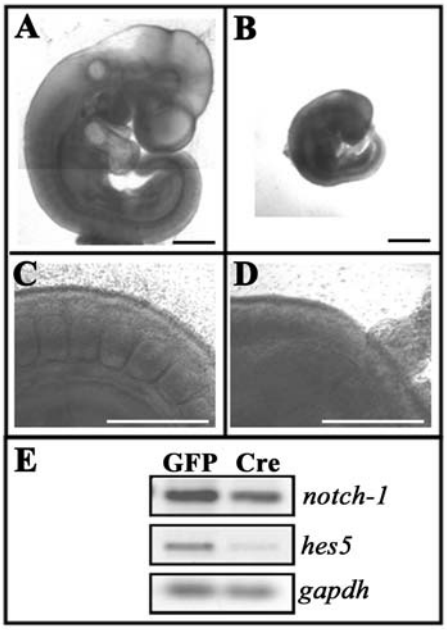

Figure II-3. Phenotype of ADAM10$^{flox\text{-}Ex9/flox\text{-}Ex9}$;CMV-Cre mice. (*A&B*) ADAM10$^{flox\text{-}Ex9/flox\text{-}Ex9}$;CMV-Cre (*B*) embryos die and are less than two-thirds the size of their littermates (*A*) at day E9.5. (*C&D*) Defect in somitogenesis observed in ADAM10$^{flox\text{-}Ex9/flox\text{-}Ex9}$;CMV-Cre embryo (*D*), but not in ADAM10$^{flox\text{-}Ex9/WT}$;CMV-Cre littermate (*C*). (Scale bar, 200 μm) Observations confirmed with at least five litters. (*E*) Semiquantitative RT-PCR showing unchanged *notch-1* transcript levels, but decreased *hes5* transcript in ADAM10$^{flox\text{-}Ex9flox\text{-}Ex9}$ MEFs infected with Ad-Cre.

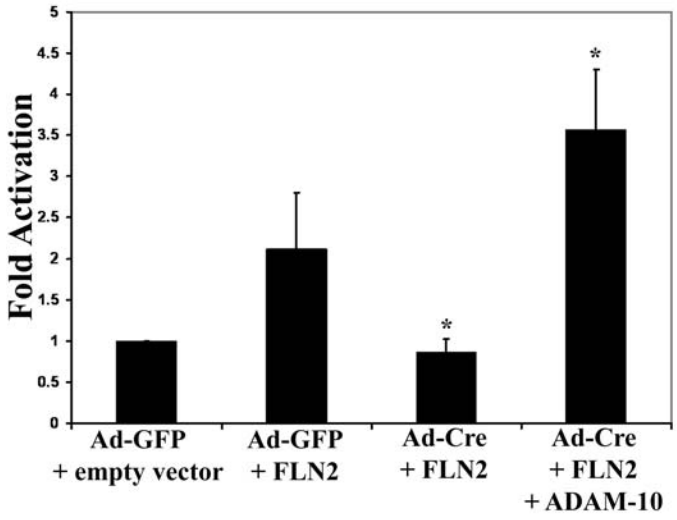

Figure II-4. Decreased Notch activity in ADAM-10$^{flox\text{-}Ex9/flox\text{-}Ex9}$ MEFs can be restored by extracellular active ADAM-10. Notch activity was assessed using a Notch-responsive promoter, containing twelve CSL binding sites. Notch activity is downregulated when ADAM-10 is removed (Ad-Cre-infected MEFs), but can be restored by the addition of cell-impermeable active ADAM-10. Data shown representing results from 4 independent experiments, with each condition assayed in triplicate during each experiment. *, $p < 0.01$, significantly different from Ad-Cre with FLN2 group.

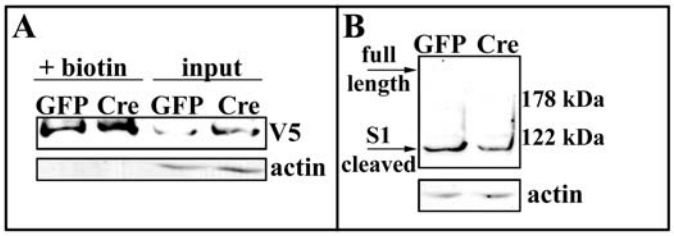

Figure II-5. ADAM-10 is not required for Notch cell surface presentation. (*A*) Cell surface biotinylation was performed in ADAM-10$^{flox\text{-}Ex9/flox\text{-}Ex9}$ MEFs infected with either Ad-GFP or Ad-Cre and transfected with Notch-2-V5. Notch-2-V5 was expressed on the cell surface, regardless of ADAM-10 expression. Blotting for actin showed that intracellular proteins were not being detected, and the input lanes show expression of Notch-2-V5 in both sets of infected MEFs. (*B*) S1 cleavage was analyzed by comparing the ratio of any full-length, monomeric Notch-2-V5 with the smaller processed form in both sets of infected MEFs. No inhibition of S1 cleavage was observed when ADAM-10 was removed. Results were confirmed over multiple experiments.

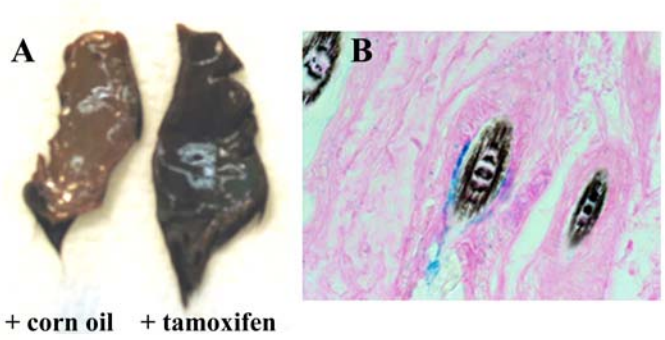

Figure II-6. Tamoxifen treatment induces Cre recombination in ROSA26R;Tyr::CreER^{T2} mice. ROSA26R;Tyr::CreER^{T2} mice were treated with tamoxifen or corn oil for 3 days, sacrificed twelve days later and their skin was harvested and stained with X-gal. (*A*) Skin from mice treated with corn oil did not stain positive, while mice treated with tamoxifen did. (*B*) Skin stained with X-gal and sectioned shows staining specifically in melanocytes, after tamoxifen treatment.

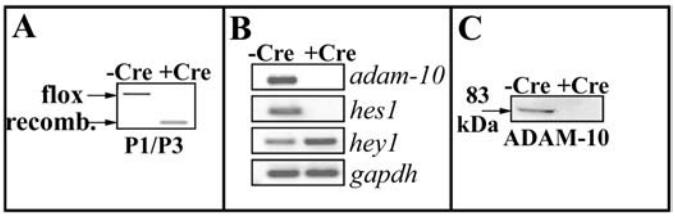

Figure II-7. ADAM-10 is conditionally removed in ADAM-10$^{flox\text{-}Ex9/flox\text{-}Ex9}$;Tyr::CreER^{T2} mice. (*A*) Genotyping of skin harvested from an ADAM-10$^{flox\text{-}Ex9/flox\text{-}Ex9}$ (-Cre) mouse and an ADAM-10$^{flox\text{-}Ex9/flox\text{-}Ex9}$;Tyr::CreER^{T2} (+Cre) mouse treated with tamoxifen. A 238 bp product obtained from primer set P1/P3 indicated Cre recombination in the skin of the ADAM-10$^{flox\text{-}Ex9/flox\text{-}Ex9}$;Tyr::CreER^{T2} mouse treated with tamoxifen. (*B*) Semiquantitative RT-PCR demonstrating loss of *adam-10*, coinciding with a loss of *hes1* and increase in *hey1*, from the skin of an ADAM-10$^{flox\text{-}Ex9/flox\text{-}Ex9}$;Tyr::CreER^{T2} mouse treated with tamoxifen. (*C*) Western blotting confirms the loss of ADAM-10 protein from the skin of an ADAM-10$^{flox\text{-}Ex9/flox\text{-}Ex9}$;Tyr::CreER^{T2} mouse treated with tamoxifen.

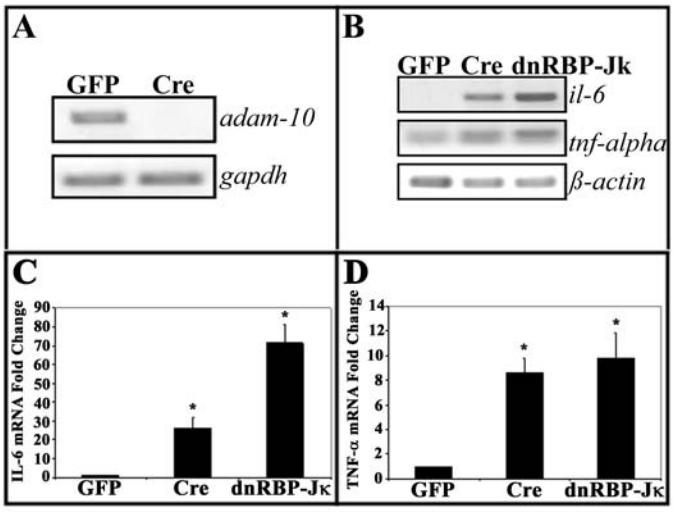

Figure II-8. The loss of ADAM10 phenocopies defective Notch signaling in primary microglia. Primary microglial cells harvested from the brains of newborn ADAM10$^{flox\text{-}Ex9/flox\text{-}Ex9}$ pups were infected with Ad-GFP, Ad-Cre or Ad-dnRBP-Jκ and activated with LPS. (*A*) Semiquantitative RT-PCR showing the loss of *adam10* in microglial cells infected with Ad-Cre. (*B-D*) Pro-inflammatory cytokines *il-6* and *tnf-α* are upregulated in activated microglial cells when *adam10* is removed (Ad-Cre-infected), and more dramatically when downstream Notch activity is perturbed (Ad-dnRBP-Jκ-infected) as determined by semiquantitative RT-PCR. Results were confirmed over multiple experiments. *, $p < 0.01$, significantly different from Ad-GFP group.

III. Miscellaneous Odds and Ends

Summary

Contained herein is what I consider interesting, yet unattached experiments. The data to follow do not necessarily flow with the previous information, but are still worth mentioning.

Development and Initial Characterization of a Primary Pancreatic Cancer Cell Line

In an attempt to establish a primary pancreatic cancer cell line, I harvested cells from an LSL-Kras$^{flox/flox}$;p48Cre pancreas. These cells would allow more detailed analysis of any signaling mechanisms observed in the LSL-Kras$^{flox/flox}$;p48Cre mouse model *in vivo*. For example, Notch signaling has been shown to be active in the pancreata of these mice, demonstrated by Hes1 positivity [66] and cleaved Notch-1 [67]. Using cells isolated from the pancreas, the Notch pathway can be manipulated, perhaps by metalloproteinase inhibitors to examine the effects of inhibition. Prospective MMP-7-specific inhibitors can be tested in order to provide insight into how effective this kind of inhibitor may be *in vivo*. In addition, other cell signaling pathways can be analyzed, including genes upregulated during the tumor progression, removing the shortcomings associated with having to analyze them in intact tissue. Here, I describe the method by which I harvested the cells, and I display the early characterization profile of the cells.

Briefly, the pancreas from a 4-month old LSL-Kras$^{flox/flox}$;p48Cre mouse was washed 3 times in 5 mL ice-cold HBSS, spinning down at 1000 rpm for 2 minutes at 4°C in between washes. The pancreas was finely minced with scissors in 2 mL HBSS, 3 mL HBSS was added, and spun down. The minced pancreas was further broken down by resuspending in 5 mL 0.2 mg/mL collagenase P, at 37°C with rocking for 15 min. Digestion was stopped by adding 5 mL ice-cold DMEM containing 10% FBS, and spinning down as above. The digested pancreas was washed 3 times in DMEM/FBS, then resuspended in 12 mL DMEM and plated onto a 6-well plate (2 mL/well). Medium was replaced the following day, aspirating large chunks present, and cells were maintained as normal thereafter.

An expression profile is shown in Figure 1A, using semi-quantitative RT-PCR. As shown, *ck-19*, *carbonic anhydrase II* (another marker of ductal cells), *amylase, notch-1*, *mmp-7* and *hes1* are expressed in the LSL-Kras$^{flox/flox}$;p48Cre cells, consistent with a tumor-filled pancreas containing metaplastic ducts. To confirm protein expression of some of these transcripts, immunofluorescence was performed for full-length Notch-1, amylase and cytokeratin (Figure 1B-D).

In conclusion, this cell line can be a useful tool for the lab, expressing our key proteins of interest.

Testing the Inhibition of MMP-7 by a Novel Inhibitor, "BSM"

I was provided with a putative metalloproteinase inhibitor generated by Francis Johnson's group (Stony Brook University), named BSM. I was asked to determine if this inhibitor is capable of inhibiting MMP-7 activity.
To test this, I included BSM in the *in vitro* MMP-7 cleavage assay (described in Materials and Methods of Chapter I), consisting of purified Notch-1-ECD peptide and active recombinant MMP-7. The BSM inhibitor effectively prevented MMP-7 from cleaving Notch at all concentrations tested: 50, 25 and 5 μg/μL (Figure 2). This is the extent of my involvement with these inhibitors.

The Serine Protease Inhibitor, Benzamidine, Prevents *In Vitro* Acinar-to-Ductal Metaplasia by Altering MMP-7 Activity

Serine proteases are involved in the activation of numerous metalloproteinases [68]. It was hypothesized that the inhibition of serine proteases may prevent MMP-7 activation, and therefore prevent ADM. To test this hypothesis, I performed an acinar cell prep and added a serine protease inhibitor, 10 mM benzamidine, along with TGF-α to the medium. Analysis on culture day 5 showed that ADM was inhibited (Figure 3A). To determine if this block of ADM was through the inhibition of MMP-7, I added either pro- or active MMP-7 (100 or 200 ng/mL, respectively) along with benzamidine and TGF-α to the culture medium. By day 5, ADM was rescued in the cells treated with active MMP-7, but not in cells treated with pro-MMP-7 (Figure 3B&C), indicating that benzamidine prevented ADM by preventing MMP-7 activation.

These results further demonstrate that MMP-7 appears to be the key enzyme responsible for *in vitro* ADM to occur. Benzamidine can prevent the activation of numerous metalloproteinases, but the inhibition of MMP-7 appears to be essential in order to prevent ADM.

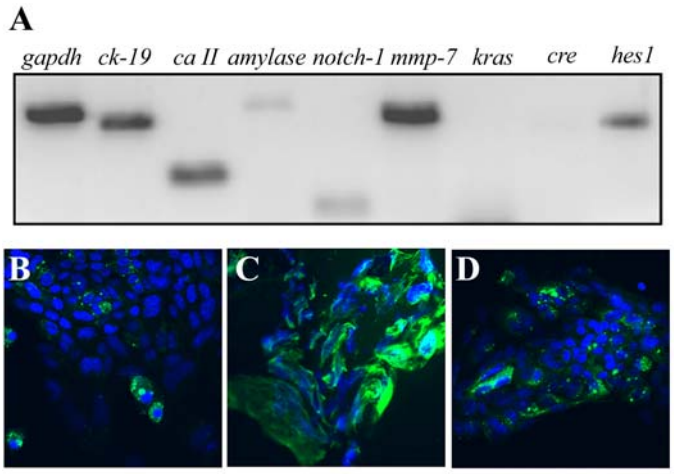

Figure III-1. Expression profile of cells harvested from an LSL-Kras$^{flox/flox}$;p48Cre pancreas. (*A*) Semiquantitative RT-PCR showing expression of *ck-19*, *carbonic anhydrase II, amylase, notch-1*, *mmp-7* and *hes1*, with *cre recombinase* slightly visible. (*B-D*) Immunofluorescence showing expression (in green) of full-length Notch-1 (*B*), cytokeratin (*C*) and amylase (*D*). DAPI shown in blue.

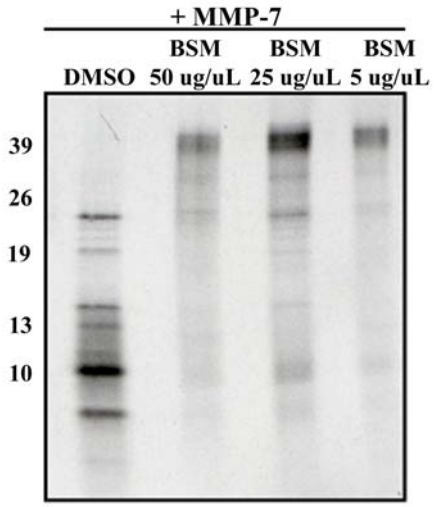

Figure III-2. Metalloproteinase inhibitor, BSM, can block MMP-7 activity *in vitro*. A peptide containing a region of Notch-1-ECD, including the metalloproteinase (P2) cleavage site, was treated with 95 ng active recombinant MMP-7 along with BSM or DMSO for 1 hour at 37°C. MMP-7 cleavage of Notch is inhibited with as little as 5 µg/µL BSM.

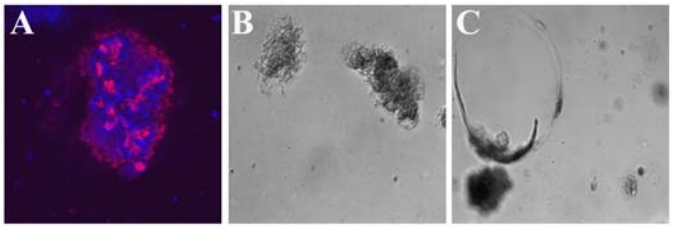

Figure III-3. Benzamidine prevents ADM by inhibiting MMP-7. (*A*) Primary acinar cells on day 5, display an acinar phenotype (amylase in red) and show no signs of ductal conversion (CK-19 in green). DAPI shown in blue. (*B&C*) Cells treated with active rMMP-7 (*C*) can bypass benzamidine inhibition and cause conversion, while cells treated with pro-MMP-7 (*B*) cannot.

IV. Final Perspective

The conditional ADAM-10 knockout mouse described here opens the door for future discovery both broadly in the field of ADAM research, as well as specifically in our lab. The obvious benefit is the ability to look at the effects of ADAM-10 removal from adult tissues. While I have been interested in ADAM-10's effect on Notch activity, its many other substrates should not be ignored. Amyloid precursor protein, EGF and betacellulin processing can all be examined now in an aged animal. The lab holds interest in pancreatic development and disease, and therefore has plans of examining ADAM-10's role specifically in the pancreas. While these experiments may prove fruitful, I think a broader view should be taken in order to take full advantage of this mouse. In addition to trying new ways of injuring the pancreas and seeing if ADAM-10 does anything, the lab should cross the conditional knockout mouse with more varied tissue-specific Cre recombinase. I have begun this approach, by using the melanocyte-specific Cre and by looking at microglial cells. Armed with such a useful tool, I think it would be detrimental to the lab not to squeeze every piece of data from this mouse, regardless of tissue. It would be interesting to identify why exactly the complete knockout mouse dies at E9.5. Removing ADAM-10 tissue by tissue may be able to answer this question; the tissue-specific Cre that kills the mouse at that age points to the tissue of interest, and numerous subsequent experiments with it. Otherwise, we will be reading about how others have observed phenotypes after simple mating.

The apparently chronic activation of Notch in the diseased pancreas together with the persistently high expression of MMP-7 in these activated epithelia suggests that MMP-7 may lead to Notch activation in a unique way, not previously seen with other metalloproteinases. In order to decipher the mechanism through which MMP-7 activates Notch, we need to more closely examine the events that initiate Notch activation. Consistent with the lateral inhibition model, in all reports pointing to either ADAM-10 or ADAM-17 as Notch's extracellular protease, Notch receptor first interacts with an adjacent ligand prior to processing. This tightly regulates Notch activity; no ligand equals no activity. Ubiquitous expression of ADAMs, coinciding with controlled systematic Notch activation, implies ligand is the key component required to regulate Notch cleavage. An important difference between MMP-7 and ADAMs is that MMP-7 expression is induced, yet it can initiate Notch activation above basal ADAM-mediated activation. Our observations that MMP-7 expression is the key step in Notch activation during ADM suggests that MMP-7 can bypass the need for ligand, cleaving Notch directly, thus removing this regulatory step of the pathway.

We propose a model in which ligand-restricted ADAM activity is essential for Notch activation during development, but increased expression of MMP-7, and probably other proteinases, causes aberrant ligand-independent Notch activation during disease progression (Fig. 1). If in fact Notch activation does not absolutely require ligand, the

possibility is introduced that Notch activation may be virtually uncontrollable in a protease-rich environment.

While the precise mechanism of how MMP-7 increases Notch activity is unknown, it is clear that both MMP-7 and Notch are important for MDLs (and by extension PDA) to form. A popular approach used to inhibit Notch is to block Notch intracellular processing by using γ-secretase inhibitors (GSI). This approach has been used by our lab, as well as by others [12], to successfully block *in vitro* ADM. Recently, others have shown that pancreatic cancer cell growth is slowed when treated with a GSI [69]. As an example in another organ system; it has been reported that GSI administration induces differentiation of intestinal adenomas in mice carrying a mutation of the Apc tumor suppressor gene [21]. Similar effects have also been reported for lung cancer [70], breast cancer [71], ovarian cancer [72] and T cell acute lymphoblastic leukemia [73]. While exciting, further progress is required to design γ-secretase inhibitors that will specifically target Notch, while not affecting other known targets. A move towards specificity has begun [74, 75], which we believe is an essential step for optimizing these drugs as potential pancreatic cancer therapeutics.

How, then, can we inhibit this activation, possibly blocking ADM and PDA *in vivo*, while avoiding the negative side effects associated with GSIs? Previous reports would suggest that ADAM-specific inhibitors would be useful to prevent Notch activation. We have demonstrated, however, that at least in the diseased pancreas, ADAM inhibition alone would be insufficient to block Notch activation, requiring a broad-spectrum approach. Treating late-stage PDA patients with broad-spectrum metalloproteinase inhibitors has proven ineffective [76], most likely due to the fact that MMPs, including MMP-7, are implicated earlier in pancreatic disease progression. Given this information, I see no reason to believe that eliminating the activity or expression of just one enzyme will prevent or reverse PDAC, in mouse or man. It will have to be a combination of numerous enzymes, most likely beyond just ADAM-10, ADAM-17 and MMP-7, discussed here. I do think the lab is on the right track creating double knockouts of MMP-7 and specific ADAMs, hopefully removing the compensatory effects we have seen thusfar *in vivo*. In order for MMP inhibitors to be useful, earlier detection, perhaps at the first signs of MDL formation, or Notch re-activation, would be required. Our finding that ADAMs are not the only proteases involved in initiating Notch signaling needs to be addressed in order to explore all avenues of Notch perturbation, and eventual tumor re-differentiation.

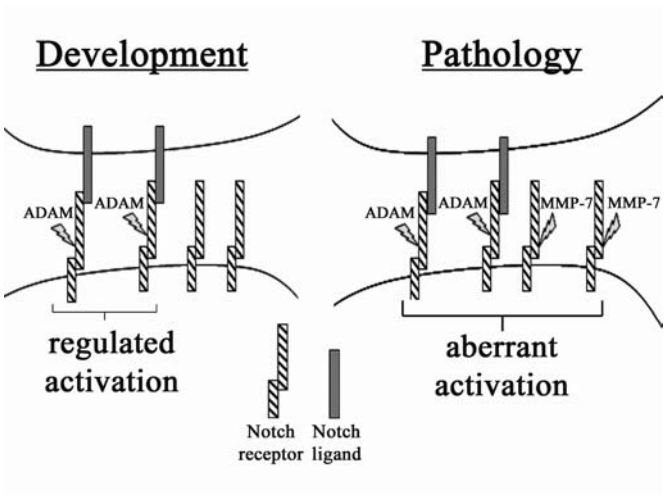

Figure IV-1. Proposed model demonstrating ligand-independent Notch activation by MMP-7. During development, Notch receptor (hatched box) interacts with ligand (gray box) and is activated by the membrane-bound ADAM metalloproteinases. In pathologies such as chronic inflammation and cancer, Notch receptor can also be activated by MMP-7 independent of the Notch receptor/ligand interaction.

References

1. *Cancer Facts and Figures 2008*. 2008 [cited; Available from: http://www.cancer.org.

2. Lowenfels AB, et al., *Pancreatitis and the risk of pancreatic cancer. International Pancreatitis Study Group.* N Engl J Med, 1993. **328**(20): p. 1433-7.

3. Lowenfels AB, et al., *Risk factors for cancer in hereditary pancreatitis. International Hereditary Pancreatitis Study Group.* Med Clin.North Am., 2000. **84**(565-573).

4. Hanck C, et al., *Cytokine gene expression in peripheral blood mononuclear cells reflects a systemic immune response in alcoholic chronic pancreatitis.* Int J Pancreatol., 1999. **26**(3): p. 137-145.

5. Marrogi A, et al., *Human mesothelioma samples overexpress both cyclooxygenase-2 (COX-2) and inducible nitric oxide synthase (NOS2): in vitro antiproliferative effects of a COX-2 inhibitor.* Cancer Res. , 2002. **60**(14): p. 3696-3700.

6. Bardeesy N, et al., *The genetics of pancreatic adenocarcinoma: a roadmap for a mouse model.* . Semin.Cancer Biol., 2001. **11**: p. 201-218.

7. Klein WM, et al., *Direct correlation between proliferation activity and dysplasia in pancreatic intraepithelial neoplasia (Pan IN): additional evidence for a recently proposed model of progression.* Mod. Pathol., 2002. **15**: p. 441-447.

8. Carriere C, et al., *The Nestin progenitor lineage is the compartment of origin for pancreatic intraepithelial neoplasia.* Proc Natl Acad Sci U S A. , 2007. **104**(11): p. 4437-4442.

9. Sandgren EP, et al., *Overexpression of TGF alpha in transgenic mice: induction of epithelial hyperplasia, pancreatic metaplasia, and carcinoma of the breast.* Cell, 1990. **61**(6): p. 1121-1135.

10. Jhappan C, et al., *TGF alpha overexpression in transgenic mice induces liver neoplasia and abnormal development of the mammary gland and pancreas.* Cell, 1990. **61**(6): p. 1137-1146.

11. Wagner M, et al., *Malignant transformation of duct-like cells originating from acini in transforming growth factor transgenic mice.* Gastoenterology, 1998. **115**(5): p. 1254-62.

12. Miyamoto Y, et al., *Notch mediates TGF alpha-induced changes in epithelial differentiation during pancreatic tumorigenesis.* Cancer Cell, 2003. **3**(6): p. 565-76.

13. Nichols JT, et al., *Notch Signaling - Constantly on the Move.* Traffic, 2007. **8**(8): p. 959-969.

14. Murtaugh LC, et al., *Notch signaling controls multiple steps of pancreatic differentiation.* Proc Natl Acad Sci U S A. , 2003. **100**(25): p. 14920-14925.

15. Esni F, et al., *Notch inhibits Ptf1 function and acinar cell differentiation in developing mouse and zebrafish pancreas.* Development, 2004. **131**(17): p. 4213-4224.

16. Beres TM, et al., *PTF1 is an organ-specific and Notch-independent basic helix-loop-helix complex containing the mammalian Suppressor of Hairless (RBP-J) or its paralogue, RBP-L.* Mol Cell Biol, 2006. **26**(1): p. 117-30.

17. Ghosh B, et al., *Interactions between hairy/enhancer of split-related proteins and the pancreatic transcription factor Ptf1-p48 modulate function of the PTF1 transcriptional complex.* Biochem J, 2006. **393**(Pt 3): p. 679-85.

18. De Lisle R, et al., *Pancreatic acinar cells in culture: expression of acinar and ductal antigens in a growth-related manner.* Eur J Cell Biol, 1990. **51**(1): p. 64-75.

19. Means AL, et al., *Pancreatic epithelial plasticity mediated by acinar cell transdifferentiation and generation of nestin-positive intermediates.* Development, 2005. **132**(16): p. 3767-76.

20. Su LK, et al., *Multiple intestinal neoplasia caused by a mutation in the murine homolog of the APC gene.* Science, 1992. **256**(5057): p. 668-670.

21. van Es JH, et al., *Notch/gamma-secretase inhibition turns proliferative cells in intestinal crypts and adenomas into goblet cells.* Nature, 2005. **435**(7044): p. 959-63.

22. Chambers AF. et al., *Changing views of the role of matrix metalloproteinases in metastasis.* J Natl Cancer Inst, 1997. **89**(17): p. 1260-70.

23. Matrisian LM, et al., *Matrix-degrading metalloproteinases in tumor progression.* Princess Takamatsu Symp, 1994. **24**: p. 152-61.

24. Powell WC, et al., *Matrilysin expression in the involuting rat ventral prostate.* Prostate, 1996. **29**(3): p. 159-68.

25. McDonnell S, et al., *Expression and localization of the matrix metalloproteinase pump-1 (MMP-7) in human gastric and colon carcinomas.* Mol Carcinog, 1991. **4**(6): p. 527-33.

26. Crawford HC, et al., *Matrix metalloproteinase-7 is expressed by pancreatic cancer precursors and regulates acinar-to-ductal metaplasia in exocrine pancreas.* J Clin Invest, 2002. **109**(11): p. 1437-44.

27. Wilson CL, et al., *Intestinal tumorigenesis is suppressed in mice lacking the metalloproteinase matrilysin.* Proc Natl Acad Sci USA, 1997. **94**(4): p. 1402-7.

28. Rudolph-Owen LA, et al., *Overexpression of the matrix metalloproteinase matrilysin results in premature mammary gland differentiation and male infertility.* Mol Biol Cell, 1998. **9**(2): p. 421-35.

29. Danielsen AJ, et al., *The EGF/ErbB receptor family and apoptosis.* Growth Factors, 2002. **20**(1): p. 1-15.

30. Li Q, et al., *Matrilysin shedding of syndecan-1 regulates chemokine mobilization and transepithelial efflux of neutrophils in acute lung injury.* Cell, 2002. **111**(5): p. 635-46.

31. Conejo JR, et al., *Syndecan-1 expression is up-regulated in pancreatic but not in other gastrointestinal cancers.* Int J Cancer, 2000. **88**(1): p. 12-20.

32. McGuire JK, et al., *Matrilysin (matrix metalloproteinase-7) mediates E-cadherin ectodomain shedding in injured lung epithelium.* Am J Pathol, 2003. **162**(6): p. 1831-43.

33. Al-Aynati MM, et al., *Epithelial-cadherin and beta-catenin expression changes in pancreatic intraepithelial neoplasia.* Clin Cancer Res, 2004. **10**(4): p. 1235-40.

34. Haro H, et al., *Matrix metalloproteinase-7-dependent release of tumor necrosis factor-alpha in a model of herniated disc resorption.* J Clin Invest. , 2000. **105**(2): p. 143-150.

35. Karayiannakis AJ, et al., *Serum levels of tumor necrosis factor-alpha and nutritional status in pancreatic cancer patients.* Anticancer Res, 2001. **21**(2B): p. 1355-8.

36. Lammich S, et al., *Constitutive and regulated alpha-secretase cleavage of Alzheimer's amyloid precursor protein by a disintegrin metalloprotease.* Proc Natl Acad Sci U S A. , 1999. **96**(7): p. 3922-3927.

37. Millichip MI, et al., *The metallo-disintegrin ADAM10 (MADM) from bovine kidney has type IV collagenase activity in vitro.* Biochem Biophys Res Commun. , 1998. **245**(2): p. 594-598.

38. Huovila AP, et al., *Shedding light on ADAM metalloproteinases.* Trends Biochem Sci. , 2005. **30**(7): p. 413-422.

39. Sotillos S, et al., *The metalloprotease-disintegrin Kuzbanian participates in Notch activation during growth and patterning of Drosophila imaginal discs.* Development, 1997. **124**(23): p. 4769-4779.

40. Lieber Y, et al., *kuzbanian-mediated cleavage of Drosophila Notch.* Genes Dev., 2002. **16**(2): p. 209-21.

41. Klein T, *kuzbanian is required cell autonomously during Notch signalling in the Drosophila wing.* Dev Genes Evol. , 2002. **212**(5): p. 251-255.

42. Pan D, et al., *Kuzbanian Controls Proteolytic Processing of Notch and Mediates Lateral Inhibition during Drosophila and Vertebrate Neurogenesis* Cell, 1997. **90**(2): p. 271-80.

43. Blaumueller CM, et al., *Intracellular cleavage of Notch leads to a heterodimeric receptor on the plasma membrane.* Cell, 1997. **90**(2): p. 281-291.

44. Brou C, et al., *A Novel Proteolytic Cleavage Involved in Notch Signaling: the Role of the Disintegrin-Metalloprotease TACE* Mol Cell, 2000. **5**(2): p. 207-16.

45. Parsa I, et al., *Ductal metaplasia of human exocrine pancreas and its association with carcinoma.* Cancer Res, 1985. **45**(3): p. 1285-90.

46. Vargo-Gogola T, et al., *Identification of novel matrix metalloproteinase-7 (matrilysin) cleavage sites in murine and human Fas ligand.* Arch Biochem Biophys. , 2002. **408**(2): p. 155-161.

47. Amour A, et al., *TNF-alpha converting enzyme (TACE) is inhibited by TIMP-3.* FEBS Lett., 1998. **435**(1): p. 39-44.

48. Hartmann D, et al., *The disintegrin/metalloprotease ADAM 10 is essential for Notch signalling but not for alpha-secretase activity in fibroblasts.* Hum Mol Genet. , 2002. **11**(21): p. 2615-24.

49. Guerra C, et al., *Chronic pancreatitis is essential for induction of pancreatic ductal adenocarcinoma by K-Ras oncogenes in adult mice.* Cancer Cell, 2007. **11**(3): p. 291-302.

50. Rodríguez CI, et al., *High-efficiency deleter mice show that FLPe is an alternative to Cre-loxP.* Nat Genet. , 2000. **25**(2): p. 139-140.

51. Kato H, et al., *Involvement of RBP-J in biological functions of mouse Notch1 and its derivatives.* Development, 1997. **124**(20): p. 4133-4141.

52. Siao CJ, TS, *Tissue plasminogen activator mediates microglial activation via its finger domain through annexin II.* J Neurosci., 2002. **22**(9): p. 3352-3358.

53. Yajima I, et al., *Spatiotemporal gene control by the Cre-ERT2 system in melanocytes.* Genesis, 2006. **44**(1): p. 34-43.

54. Gu H, et al., *Independent control of immunoglobulin switch recombination at individual switch regions evidenced through Cre-loxP-mediated gene targeting.* Cell, 1993. **73**(6): p. 1155-1164.

55. Schwenk F, et al., *A cre-transgenic mouse strain for the ubiquitous deletion of loxP-flanked gene segments including deletion in germ cells.* Nucleic Acids Res. , 1995. **23**(24): p. 5080-5081.

56. Soriano, P, *Generalized lacZ expression with the ROSA26 Cre reporter strain.* Nat Genet. , 1999. **21**(1): p. 70-71.

57. Bosenberg M, et al., *Characterization of melanocyte-specific inducible Cre recombinase transgenic mice.* Genesis, 2006. **44**(5): p. 262-267.

58. Grandbarbe L, et al., *Notch signaling modulates the activation of microglial cells.* Glia, 2007. **55**(15): p. 1519-1530.

59. Moriyama M, et al., *Notch signaling via Hes1 transcription factor maintains survival of melanoblasts and melanocyte stem cells.* J Cell Biol. , 2006. **173**(3): p. 333-339.

60. Schouwey K, et al., *Notch1 and Notch2 receptors influence progressive hair graying in a dose-dependent manner.* Dev Dyn. , 2007. **236**(1): p. 282-289.

61. Peschon JJ, et al., *An essential role for ectodomain shedding in mammalian development.* Science, 1998. **282**(5392): p. 1281-1284.

62. Katoh M, et al., *Integrative genomic analyses on HES/HEY family: Notch-independent HES1, HES3 transcription in undifferentiated ES cells, and Notch-*

dependent HES1, HES5, HEY1, HEY2, HEYL transcription in fetal tissues, adult tissues, or cancer. Int J Oncol. , 2007. **31**(2): p. 461-466.

63. Berechid BE, et al., *Lack of requirement for presenilin1 in Notch1 signaling.* Curr Biol. , 1999. **9**(24): p. 1493-1496.

64. Herreman A, et al., *Presenilin 2 deficiency causes a mild pulmonary phenotype and no changes in amyloid precursor protein processing but enhances the embryonic lethal phenotype of presenilin 1 deficiency.* Proc Natl Acad Sci U S A., 1999. **96**(21): p. 11872-11877.

65. Six E, et al., *The Notch ligand Delta1 is sequentially cleaved by an ADAM protease and gamma-secretase.* Proc Natl Acad Sci U S A. , 2003. **100**(13): p. 7638-7643.

66. Hingorani SR, et al., *Preinvasive and invasive ductal pancreatic cancer and its early detection in the mouse.* Cancer Cell, 2003. **4**(6): p. 437-450.

67. Sawey ET, et al., *Metalloproteinases and cell fate: Notch just ADAMs anymore.* Cell Cycle, 2007. **7**(5): p. 566-569.

68. Leach SD, et al., *Intracellular activation of digestive zymogens in rat pancreatic acini. Stimulation by high doses of cholecystokinin.* J Clin Invest. , 1991. **87**(1): p. 362-366.

69. Kimura K, et al., *Activation of Notch signaling in tumorigenesis of experimental pancreatic cancer induced by dimethylbenzanthracene in mice.* Cancer Sci., 2007. **98**(2): p. 155-162.

70. Konishi J, et al., *Gamma-secretase inhibitor prevents Notch3 activation and reduces proliferation in human lung cancers.* Cancer Res., 2007. **67**(17): p. 8051-8057.

71. Zang S, et al., *A study on Notch signaling in human breast cancer.* Neoplasma., 2007. **54**(4): p. 304-310.

72. Park JT, et al., *Notch3 gene amplification in ovarian cancer.* Cancer Res, 2006. **66**(12): p. 6312-6318.

73. Lewis HD, et al., *Apoptosis in T cell acute lymphoblastic leukemia cells after cell cycle arrest induced by pharmacological inhibition of notch signaling.* Chem Biol, 2007. **14**(2): p. 209-219.

74. Zhao B, et al., *Identification of gamma -secretase inhibitor potency determinants on Presenilin.* J Biol Chem., 2007. **283**(5): p.2927-2938.

75. Best JD, et al., *The novel gamma secretase inhibitor N-[cis-4-[(4-chlorophenyl)sulfonyl]-4-(2,5-difluorophenyl)cyclohexyl]-1,1,1-trifluoromethanesulfonamide (MRK-560) reduces amyloid plaque deposition without evidence of notch-related pathology in the Tg2576 mouse.* J Pharmacol Exp Ther. , 2007. **320**(2): p. 552-558.

76. Bramhall SR, et al.; Marimastat Pancreatic Cancer Study Group, *Marimastat as first-line therapy for patients with unresectable pancreatic cancer: a randomized trial.* J Clin Oncol. , 2001. **19**(15): p. 3447-3455.

Appendix 1 – Primers Used

gene	forward primer (5'-3')	reverse primer (5'-3')
mmp-7	AGGGTTAGTTGGGGGACTGCGGATATC	GGAGGACCCAGTGAGTGCAGACCGTT
hes1	AAAGACGGCCTCTGAGCACA	TCATGGCGTTGATCTGGGTCA
hey1	TGGGGACCTAGACTACCAGC	CCACCCTAAAGTCGCCAGTA
notch-1	CGGTGAACAATGTGGATGCT	ACTTTGGCAGTCTCATAGCT
adam-10	GATGAAAAAGACCCTACAAATCCTTTCC	GTAATTGCCATTTTCTTTTTGTCCTAAGTT
hes5	CAAGGAGAAAAACCGACTGC	GCTGGAAGTGGTAAAGCAGC
hey1	TGGGGACCTAGACTACCAGC	CCACCCTAAAGTCGCCAGTA
adam-9	CCAGACCCAGGGATGGTGAAT	GGCCATGACATTTTCCCTGAA
adam-17	TGATTCTTTGCTCTCAGAC	GTTGATTCTCACTGTAACATC
tnf-α	CTCCCTCCAGAAAAGACACC	TTTGGGGACCGATCACCCCG
β-actin	CGTGGGCCGCCCTAGGCACCA	TTGGCCTTAGGGTTCAGGGGGG
il-6	TGCCTTCTTGGGACTGATGC	GCCTCCGACTTGTGAAGTGG
ck-19	GGGTCAGGGGGTGTTTTCCGCGCAC	ATTGTCAATCTGTAGGACAATCTTGGAGTT
carbonic anhydrase II	AGATTGGACCTGCCTCACAA	TGCTCGCTGCTGACAGTAAT
amylase	GGAATGTGAGCGATACTTAGCTCCTAAGGGA	CGAACATAATCTTTCTCAAGTGCAAGATCC
adam-10 Δneo/wild type	GTTGGACATAACTTTGGATCTCC	CGTATCTCAAAACTACCCTCCC
recombined *adam-10*	GAAGGGATATAAGCTTTGGTTCAGTG	CGTATCTCAAAACTACCCTCCC
cre recombinase	ACCTGAAGATGTTCGCGATTATCT	ACCGTCAGTACGTGAGATATCTT